Article

Journal of Vibration and Control
1–19

DOI: 10.1177/1077546316655706
jvc.sagepub.com
SAGE

On averaging and input optimization of high-frequency mechanical control systems

Sevak Tahmasian[1], David W Allen[2] and Craig A Woolsey[2]

Abstract

This paper presents the optimization of input amplitudes for mechanical control-affine systems with high-frequency, high-amplitude inputs. The problem consists of determining the input waveform shapes and the relative phases between inputs to minimize the input amplitudes while accomplishing some control objective. The effects of the input waveforms and relative phases on the dynamics are investigated using averaging. It is shown that of all zero-mean, periodic functions, square waves require the smallest amplitudes to accomplish a control objective. Using the averaging theorem the problem of input optimization is transformed into a constrained optimization problem. The constraints are algebraic nonlinear equalities in terms of the amplitudes of the inputs and their relative phases. The constrained optimization problem may be solved using analytical or numerical methods. A second approach uses finite Fourier series to solve the input optimization problem. This second approach confirms the earlier results concerning minimum amplitude inputs and is then applied to the problem of minimizing control energy.

Keywords

Vibrational control, input optimization, averaging, control-affine systems, nonlinear control

1. Introduction

The actuators for mechanical control systems provide the necessary forces and moments to generate desired motions. The mass of an actuator scales with its maximum output. Thus, control forces with large amplitudes require bigger actuators which increases the total mass of the system. Besides minimizing the energy or time required for a system to accomplish a task (Bobrow et al., 1985; Berman and Wang, 2007; Gregory et al., 2012), designers are often interested in minimizing the total mass of a robotic system (Chedmail and Gautier, 1990). For biomimetic robots such as flapping wing micro air vehicles (FWMAVs), decreasing the total mass of the system is an especially important design objective (Karpelson et al., 2008).

Many robotic systems can be modeled as mechanical systems that are affine in their inputs. Mechanical control-affine systems may use high-frequency periodic inputs to effect desired motions "on average" (Bullo, 2002; Bullo and Lewis, 2005). Control of mechanical systems using high- (force) amplitude, high-frequency inputs is known as "vibrational control" (Meerkov, 1977; Bellman et al., 1986a, b). One of the simplest examples of using vibrational control for stabilization is the Stephenson–Kapitza pendulum (Kapitza, 1965), a two-degree-of-freedom (2-DOF) inverted pendulum that is stabilized by high-frequency vertical oscillations of its pivot. More complex examples are biological and biomimetic systems such as insects, small birds, real and robotic fish, and FWMAVs. These systems use high-frequency flapping of their wings, tails, and fins to fly or swim or to perform desired motions (Wood, 2008; Oppenheimer et al., 2011; Anderson and Cobb, 2012).

The averaging theorem is a useful tool for analyzing the dynamics of time-periodic systems (Guckenheimer

[1]Department of Biomedical Engineering and Mechanics, Virginia Tech, USA
[2]Department of Aerospace and Ocean Engineering, Virginia Tech, USA

Received: 1 September 2015; accepted: 27 May 2016

Corresponding author:
Sevak Tahmasian, 223 Norris Hall, 495 Old Turner Street, Blacksburg, VA 24061, USA.
Email: sevakt@vt.edu

and Holmes, 1983; Sanders and Verhulst, 1985). Applying averaging to a time-periodic system yields time-invariant dynamics that can be used to analyze the time-varying system. Using the averaging theorem and the nonlinear variation of constants formula, (Bullo, 2002) presented an averaging technique for vibrational control systems.

This paper addresses minimizing the input amplitude for a class of mechanical control-affine systems with high-frequency, high-amplitude zero-mean inputs, using the averaging technique described in (Bullo and Lewis, 2005). After discussing the effects of the relative phase of the inputs on the averaged dynamics, it is shown that the averaged dynamics do not change if all the inputs are shifted by the same amount. It is then shown that, of all zero-mean, periodic inputs that generate the same averaged dynamics, a square wave has the smallest amplitude. The input optimization problem is then transformed into a classical constrained optimization problem (Bertsekas, 1982; Burns, 2014). A set of algebraic nonlinear equality constraints is derived that must be satisfied by the optimum inputs. The independent parameters appearing in the equality constraints are the amplitudes of the square inputs and their relative phases. Next, a finite Fourier series approach to input optimization is presented. In this approach the cost functional is determined using a finite Fourier series representation of the zero-mean periodic inputs. An example of a 3-DOF mechanical control system shows agreement with the earlier, analytical results. The finite Fourier series approach is then applied to the problem of minimizing the input energy.

For the averaging theorem to be applicable, the operation frequency of the vibrational system must exceed some minimum value ω_0 which depends on the physics and parameters of the system, and input amplitudes. If the forcing frequency exceeds this minimum value then the averaging theorem guarantees that if there is a hyperbolically stable equilibrium of the averaged system dynamics, there is a corresponding, hyperbolically stable periodic orbit for the original system. Currently there is no general analytical method to determine the value of ω_0. Therefore in this paper we simply assume that the forcing frequency is higher than ω_0, whatever its value. We also assume that by changing the input amplitudes the forcing frequency still remains higher than the ω_0 corresponding to the new input amplitudes. Meerkov (1973) presented an equation to estimate the minimum frequency ω_0 for a system, but it results in a conservative value (Bellman et al., 1985). Using stability maps, Berg and Wickramasinghe (2015) have shown that for (possibly narrow) ranges of frequencies less than ω_0, the original system may still possess stable periodic orbits. These stabilizing ranges of frequencies, if they exist, are not predicted by the averaging theorem and may be determined using numerical methods.

The paper is organized as follows. In Section 2, after reviewing the averaging theorem as applied to vibrational control systems, the effects of phase shifting of the inputs on the averaged dynamics are discussed. In Section 3, the effects of the input waveform shape are considered and an optimization problem for a 1-DOF example is solved. Input optimization for higher-dimensional systems, along with examples, are presented in Section 4. Section 5 presents a numerical approach to solve the input optimization problem using a finite Fourier series representation of the input waveforms. Energy optimization using the finite Fourier series is discussed in Section 6. Section 7 summarizes the contributions.

2. Averaging of mechanical control-affine systems

Consider the time-periodic dynamical system

$$\dot{\boldsymbol{x}} = \epsilon \boldsymbol{f}(\boldsymbol{x}, t), \quad \boldsymbol{x}(0) = \boldsymbol{x}_0 \tag{1}$$

where $\boldsymbol{f}(\boldsymbol{x},t)$ is T-periodic in its second argument and $\epsilon > 0$ is a small number. The averaged dynamics of the system in equation (1) is defined as (Guckenheimer and Holmes, 1983; Sanders and Verhulst, 1985)

$$\dot{\bar{\boldsymbol{x}}} = \epsilon \bar{\boldsymbol{f}}(\bar{\boldsymbol{x}}), \quad \bar{\boldsymbol{x}}(0) = \boldsymbol{x}_0 \tag{2}$$

where

$$\bar{\boldsymbol{f}}(\bar{\boldsymbol{x}}) = \frac{1}{T}\int_0^T \boldsymbol{f}(\bar{\boldsymbol{x}}, t)\mathrm{d}t$$

According to the averaging theorem if $\boldsymbol{x}(t)$ and $\bar{\boldsymbol{x}}(t)$ are solutions of equation (1) and equation (2) respectively, then $\boldsymbol{x}(t) = \bar{\boldsymbol{x}}(t) + O(\epsilon)$ on a time scale $\frac{1}{\epsilon}$. Moreover, if $\bar{\boldsymbol{x}}_\mathrm{e}$ is a hyperbolic equilibrium point of equation (2), then there exists $\epsilon_0 > 0$ such that for all $0 < \epsilon \leq \epsilon_0$, the system in equation (1) possesses a unique hyperbolic periodic orbit $\boldsymbol{x}_\mathrm{p}(t) = \bar{\boldsymbol{x}}_\mathrm{e} + O(\epsilon)$ of the same stability type as $\bar{\boldsymbol{x}}_\mathrm{e}$ (Guckenheimer and Holmes, 1983; Sanders and Verhulst, 1985).

The dynamics of an n-DOF mechanical control-affine system with m inputs can be written in the following form

$$\ddot{\boldsymbol{q}} = \boldsymbol{f}(\boldsymbol{q}, \dot{\boldsymbol{q}}) + \sum_{i=1}^{m} \boldsymbol{g}_i(\boldsymbol{q})u_i(t), \quad \boldsymbol{q}(0) = \boldsymbol{q}_0, \quad \dot{\boldsymbol{q}}(0) = \boldsymbol{v}_0 \tag{3}$$

where $\boldsymbol{q} = (q_1, \ldots, q_n)^T$ is the vector of generalized coordinates and $u_i(t)$ are the inputs. For each

$i \in \{1, \ldots, m\}$, take $u_i(t)$ to be the following high-frequency, high-amplitude input

$$u_i(t) = \omega v_i(\omega t) \tag{4}$$

where ω is the (high) frequency, and $v_i(t)$ is a zero-mean, T-periodic function.

Defining the state vector $\boldsymbol{x} = (\boldsymbol{q}^{\mathrm{T}}, \ \dot{\boldsymbol{q}}^{\mathrm{T}})^{\mathrm{T}}$ and using the inputs defined in equation (4), the system in equation (3) can be written in the first order form

$$\dot{\boldsymbol{x}} = \boldsymbol{Z}(\boldsymbol{x}) + \sum_{i=1}^{m} \boldsymbol{Y}_i(\boldsymbol{x})\left(\frac{1}{\epsilon}\right) v_i\left(\frac{t}{\epsilon}\right), \boldsymbol{x}(0) = \boldsymbol{x}_0 = (\boldsymbol{q}_0^{\mathrm{T}}, \boldsymbol{v}_0^{\mathrm{T}})^{\mathrm{T}} \tag{5}$$

where $\epsilon = \frac{1}{\omega}$, $\boldsymbol{Z}(\boldsymbol{x}) = \left(\dot{\boldsymbol{q}}^{\mathrm{T}}, \ \boldsymbol{f}^{\mathrm{T}}(\boldsymbol{q}, \dot{\boldsymbol{q}})\right)^{\mathrm{T}}$ is the drift vector field, and $\boldsymbol{Y}_i(\boldsymbol{x}) = \left(\boldsymbol{0}_{1\times n}, \ \boldsymbol{g}_i^{\mathrm{T}}(\boldsymbol{q})\right)^{\mathrm{T}}$ are the input vector fields.

Following the discussion in Bullo and Lewis (2005: Chapter 9), for the inputs in equation (4), we define scalar parameters κ_i, λ_{ij}, and μ_{ij}, for $i,j \in \{1, \ldots, m\}$, as follows

$$\kappa_i = \frac{1}{T}\int_0^T \int_0^t v_i(\tau)\mathrm{d}\tau \, \mathrm{d}t \tag{6}$$

$$\lambda_{ij} = \frac{1}{T}\int_0^T \left(\int_0^t v_i(\tau)\mathrm{d}\tau\right)\left(\int_0^t v_j(\tau)\mathrm{d}\tau\right)\mathrm{d}t \tag{7}$$

and

$$\mu_{ij} = \frac{1}{2}(\lambda_{ij} - \kappa_i\kappa_j) \tag{8}$$

Also we define the *symmetric product* between two input vector fields $\boldsymbol{Y}_i(\boldsymbol{x})$ and $\boldsymbol{Y}_j(\boldsymbol{x})$ as

$$\langle \boldsymbol{Y}_i : \boldsymbol{Y}_j \rangle(\boldsymbol{x}) = \langle \boldsymbol{Y}_j : \boldsymbol{Y}_i \rangle(\boldsymbol{x}) = \left[\boldsymbol{Y}_j(\boldsymbol{x}), [\boldsymbol{Z}(\boldsymbol{x}), \boldsymbol{Y}_i(\boldsymbol{x})]\right] \tag{9}$$

where $[\cdot,\cdot]$ denotes the Lie bracket of vector fields.

Therom 1. (*Adapted from* (*Bullo and Lewis* (2005)): *Consider the control-affine system in equation* (3) *with high-frequency, high-amplitude inputs defined as equation* (4), *and its first order form in equation* (5). *Suppose that* $\boldsymbol{f}(\boldsymbol{q}, \dot{\boldsymbol{q}})$ *and* $\boldsymbol{g}_i(\boldsymbol{q})$ *depend polynomially on their arguments, are twice differentiable in* $\boldsymbol{q}$, *and that the components of* $\boldsymbol{f}(\boldsymbol{q}, \dot{\boldsymbol{q}})$ *are homogeneous in* $\dot{\boldsymbol{q}}$ *of degree two and less. Consider the time-invariant system*

$$\dot{\bar{\boldsymbol{x}}} = \boldsymbol{Z}(\bar{\boldsymbol{x}}) - \sum_{i,j=1}^{m} \mu_{ij} \langle \boldsymbol{Y}_i : \boldsymbol{Y}_j \rangle(\bar{\boldsymbol{x}}) \tag{10}$$

with the initial condition $\bar{\boldsymbol{x}}(0) = \bar{\boldsymbol{x}}_0 = \boldsymbol{x}_0 + \sum_{i=1}^{m} \kappa_i \boldsymbol{Y}_i(\boldsymbol{x}_0)$, *where* $\bar{\boldsymbol{x}} = (\bar{\boldsymbol{q}}^{\mathrm{T}}, \ \dot{\bar{\boldsymbol{q}}}^{\mathrm{T}})^{\mathrm{T}}$ *is the state vector. There exists a positive* ϵ_0 *(corresponding to a frequency* ω_0*) such that for all* $0 < \epsilon \leq \epsilon_0$ *(equivalently,* $\omega \geq \omega_0$*),* $\boldsymbol{q}(t) = \bar{\boldsymbol{q}}(t) + O(\epsilon)$ *as* $\epsilon \to 0$ *on the time scale 1. Furthermore, if the system in equation (10) possesses a hyperbolically stable equilibrium point* $\bar{\boldsymbol{x}}_{\mathrm{e}}$, *then the system in equation* (5) *possesses a hyperbolically stable periodic orbit within an* $O(\epsilon)$ *neighborhood of the equilibrium point* $\bar{\boldsymbol{x}}_{\mathrm{e}}$, *and the approximation* $\boldsymbol{q}(t) = \bar{\boldsymbol{q}}(t) + O(\epsilon)$ *is valid for all time* $t \geq 0$.

We call the time-invariant system in equation (10) the averaged form of the time-periodic system in equation (5).

Remark 2. *Note that since the first n components of the input vector fields* $\boldsymbol{Y}_i(\boldsymbol{x})$, $i \in \{1, \ldots, m\}$, *are zero, the initial conditions of the averaged dynamics in equation* (10) *may also be written as* $\bar{\boldsymbol{q}}(0) = \boldsymbol{q}_0$ *and* $\dot{\bar{\boldsymbol{q}}}(0) = \boldsymbol{v}_0 + \sum_{i=1}^{m} \kappa_i \boldsymbol{g}_i(\boldsymbol{q}_0)$.

Therom 3. *Consider the two control-affine systems in equation* (5) *and equation* (11) *below*

$$\dot{\boldsymbol{y}} = \boldsymbol{Z}(\boldsymbol{y}) + \sum_{i=1}^{m} \boldsymbol{Y}_i(\boldsymbol{y})\left(\frac{1}{\epsilon}\right) w_i\left(\frac{t}{\epsilon}\right), \quad \boldsymbol{y}(0) = \boldsymbol{x}_0 \tag{11}$$

where $w_i(t) = v_i(t + \phi_0)$, $i \in \{1, \ldots, m\}$, *and* $0 \leq \phi_0 \leq T$. *For any* $\phi_0 \in [0, T]$, *the systems in equation* (11) *and equation* (5) *have identical averaged dynamics with different initial states.*

Proof. See Appendix 1.

The claim in Theorem 3 does not hold if the phase shift is not applied uniformly, that is, if the phase of one input is shifted relative to another. In this case, the stability properties of the averaged and original dynamics may also be affected. To make this clear, we present the following example.

Example 1. Consider the following mechanical system with two inputs

$$\dot{\boldsymbol{x}} = \underbrace{\begin{pmatrix} x_3 \\ x_4 \\ x_3^2 - x_4^2 - x_3 + x_1 - x_2 \\ x_3^2 + x_4^2 - 0.8x_4 - 3x_1 \end{pmatrix}}_{\boldsymbol{Z}(\boldsymbol{x})} + \underbrace{\begin{pmatrix} 0 \\ 0 \\ 2x_2 \\ 0 \end{pmatrix}}_{\boldsymbol{Y}_1(\boldsymbol{x})} \omega v_1(\omega t) + \underbrace{\begin{pmatrix} 0 \\ 0 \\ 0 \\ 3x_1 \end{pmatrix}}_{\boldsymbol{Y}_2(\boldsymbol{x})} \omega v_2(\omega t) \tag{12}$$

Considering the inputs $v_1(t) = \cos t$ and $v_2(t) = \cos(t + \phi_0)$, where $0 \le \phi_0 \le 2\pi$, and using equation (6) through equation (8), one determines $\kappa_1 = 0$, $\kappa_2 = -\sin\phi_0$, $\mu_{11} = \mu_{22} = \frac{1}{4}$ and $\mu_{12} = \mu_{21} = \frac{1}{4}\cos\phi_0$. Using Theorem 1, the averaged dynamics of equation (12) are

$$\begin{cases} \dot{\bar{x}}_1 = \bar{x}_3 \\ \dot{\bar{x}}_2 = \bar{x}_4 \\ \dot{\bar{x}}_3 = \bar{x}_3^2 - \bar{x}_4^2 - \bar{x}_3 - 4.5\bar{x}_1^2 + 2\bar{x}_2^2 + (1 - 3\cos\phi_0)\bar{x}_1 - \bar{x}_2 \\ \dot{\bar{x}}_4 = \bar{x}_3^2 + \bar{x}_4^2 - 0.8\bar{x}_4 + 4.5\bar{x}_1^2 + 2\bar{x}_2^2 - 3\bar{x}_1 - 3\bar{x}_2\cos\phi_0 \end{cases} \tag{13}$$

where $\bar{\boldsymbol{x}} = (\bar{x}_1,\ \bar{x}_2,\ \bar{x}_3,\ \bar{x}_4)^{\mathrm{T}}$ is the state vector of the averaged dynamics. The origin is an equilibrium point of the original system in equation (12) and of its averaged dynamics in equation (13). Linearizing the averaged dynamics in equation (13) about the origin, one obtains the linear, time-invariant system

$$\boldsymbol{\delta}\dot{\bar{\boldsymbol{x}}} = \begin{pmatrix} 0 & 0 & 1 & 0 \\ 0 & 0 & 0 & 1 \\ 1 - 3\cos\phi_0 & -1 & -1 & 0 \\ -3 & -3\cos\phi_0 & 0 & -0.8 \end{pmatrix} \boldsymbol{\delta}\bar{\boldsymbol{x}} \tag{14}$$

where $\boldsymbol{\delta}\bar{\boldsymbol{x}}$ is the state vector of the linearized averaged system. Using the eigenvalues of the state matrix of the linearized system it can be shown that the linear system in equation (14) is unstable for $0.696 < \phi_0 < 5.588$, and stable otherwise. Therefore the time-periodic system in equation (12) possesses an unstable periodic orbit about the origin for $0.696 < \phi_0 < 5.588$, and a stable one otherwise.

A portrait of the root locus of the linearized system in equation (14) when changing ϕ_0 is shown in Figure 1(a). The responses of the original time-periodic system and its averaged dynamics for $\phi_0 = 0$ and $\phi_0 = 0.733$ are presented in Figure 1(c) and (d). The initial conditions for the simulations are $\boldsymbol{x}(0) = (0.1, -0.1, 0, 0)^T$, and $\omega = 50$. Note that since the state matrix of the linear system varies with $\cos\phi_0$, which is bounded, the branches of the root locus of the linear system shown in Figure 1(a) have finite lengths; none approaches infinity.

In Figure 1(d), though the origin is an unstable equilibrium point, the new equilibrium point that emerges from the bifurcation is stable for $\phi_0 \le 1.434$ and $\phi_0 \ge 4.849$; see Figure 1(b). Therefore, for $\phi_0 = 0.733$, the averaging results are still valid, except that the stability predictions correspond to a shifted equilibrium point.

3. Input optimization of 1-DOF control-affine systems

Consider the system in equation (3) where $m = n = 1$. Using q as the generalized coordinate, $\boldsymbol{x} = (q, \dot{q})^{\mathrm{T}}$ as the state vector, and the high-frequency, high-amplitude input $u_1(t) = \omega v_1(\omega t)$, where $v_1(t)$ is a T-periodic, zero-mean function, the first order form can be written as

$$\dot{\boldsymbol{x}} = \boldsymbol{Z}(\boldsymbol{x}) + \boldsymbol{Y}(\boldsymbol{x})\omega v_1(\omega t) \tag{15}$$

where $\boldsymbol{Z}(\boldsymbol{x})$ and $\boldsymbol{Y}(\boldsymbol{x})$ are defined as for equation (5). The goal is to find the input function $v_1(t)$ with the minimum amplitude for the system in equation (15) to have a stable periodic orbit in an $O(\epsilon)$ neighborhood of a point $\boldsymbol{x}_e = (q_e, 0)$, where $\epsilon = \frac{1}{\omega}$.

Remark 4. *In this and subsequent sections, we only consider vibrational control systems operating with a forcing frequency that is sufficiently high for the averaging theorem to apply. In terms of Theorem 1, we assume that $\epsilon \le \epsilon_0$, or $\omega \ge \omega_0$.*

Using Theorem 1, the averaged dynamics of equation (15) can be written as

$$\dot{\bar{\boldsymbol{x}}} = \boldsymbol{Z}(\bar{\boldsymbol{x}}) - \mu_{11}\langle \boldsymbol{Y} : \boldsymbol{Y}\rangle(\bar{\boldsymbol{x}}) \tag{16}$$

where μ_{11} can be determined using equation (8). Thus the parameter μ_{11}, associated with the input $v_1(t)$, serves to scale the influence of the symmetric product. According to Theorem 1, if the averaged dynamics in equation (16) has an exponentially stable equilibrium point at $\bar{\boldsymbol{x}}_e$, then the time-periodic system in equation (15) has an exponentially stable periodic orbit in an $O(\epsilon)$ neighborhood of $\bar{\boldsymbol{x}}_e$. To begin, we require that the point $\boldsymbol{x}_e$ be an equilibrium point of the averaged dynamics in equation (16), i.e.

$$\boldsymbol{0} = \boldsymbol{Z}(\boldsymbol{x}_e) - \mu_{11}\langle \boldsymbol{Y} : \boldsymbol{Y}\rangle(\boldsymbol{x}_e) \tag{17}$$

The set of equations (17) consists of two algebraic equations. The first of these two equations is automatically satisfied because the second component of $\boldsymbol{x}_e$ (the velocity component, $\dot{q}$) is zero. The second of these equations can be written as

$$f(q_e, 0) - \mu_{11}h(q_e) = 0 \tag{18}$$

where $h(q_e) = \boldsymbol{e}_2 \cdot \langle \boldsymbol{Y} : \boldsymbol{Y}\rangle\,(q_e)$, and $\boldsymbol{e}_i$ is the ith unit vector of the standard basis of Euclidean space (i.e. $\boldsymbol{e}_2 = (0, 1)^T$). Assuming that $h(q_e)$ is nonzero, $\bar{\boldsymbol{x}}_e = \boldsymbol{x}_e$ will be an equilibrium of the averaged dynamics provided

$$\mu_{11} = \frac{f(q_e, 0)}{h(q_e)} \tag{19}$$

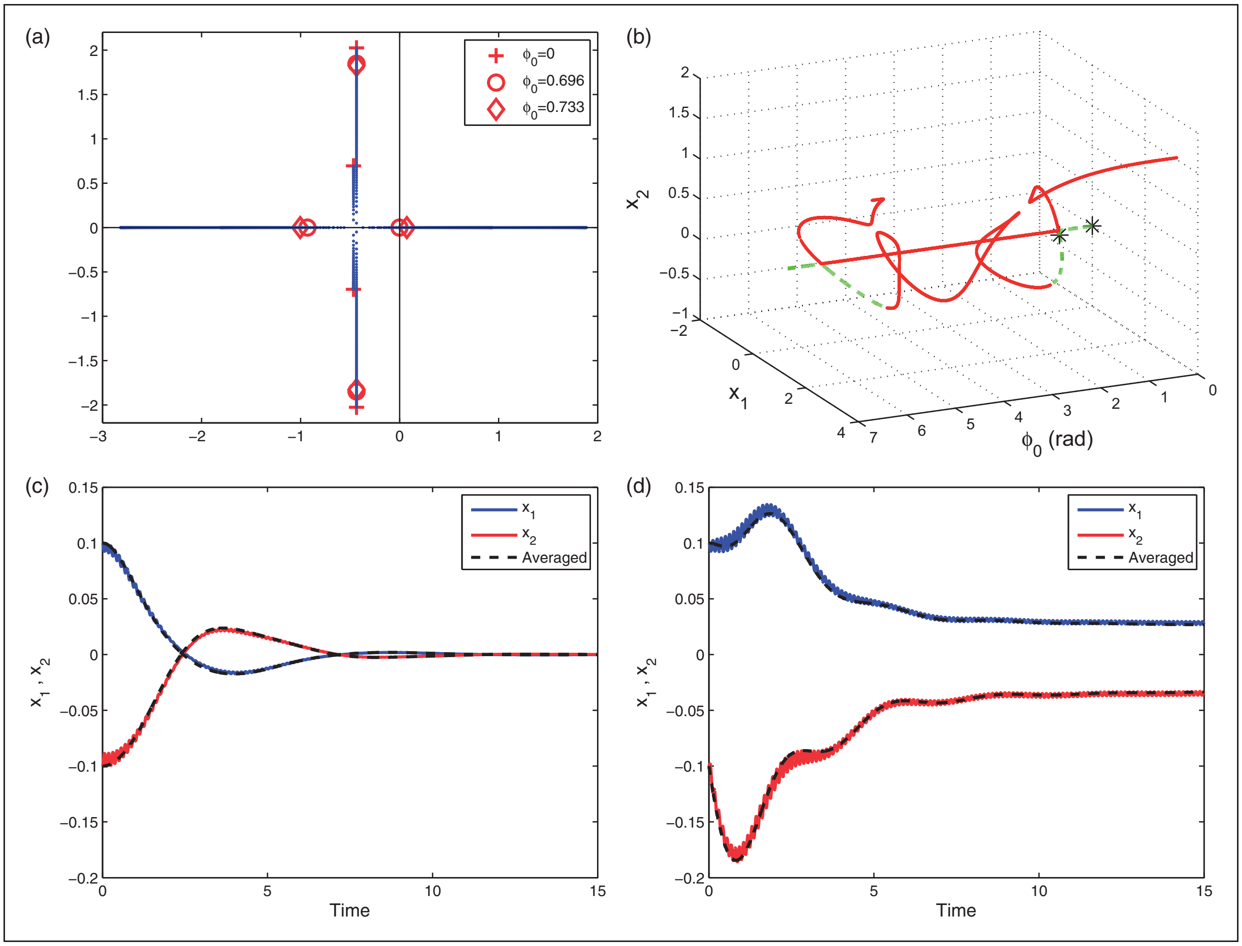

Figure 1. Root locus (a) and bifurcation diagram (b) for $\phi_0 \in [0, 2\pi]$ along with time histories for the original and time-averaged dynamics with $\phi_0 = 0$ (c) and $\phi_0 = 0.733$ (d). The equilibria in (c) and (d) are denoted by black asterisks in (b). Dashed-green and full-red in (b) represent stable and unstable equilibria of (13), respectively.

The parameter μ_{11} determined using equation (19) only guarantees that q_e is an equilibrium of the averaged system in equation (16). But it does not guarantee the stability of the equilibrium point q_e. Ensuring that the equilibrium is exponentially stable requires additional analysis and, in some cases, feedback control as described in (Tahmasian and Woolsey, 2015).

Remark 5. *For some systems, the origin is an equilibrium point of both the time-varying system and its averaged dynamics. For bilinear systems such as the following, for example, the origin is an equilibrium regardless of the input* (Martinez et al., 2003)

$$\ddot{q} = f_0(q, \dot{q})q + g_0(q)qu(t)$$

Using input $u(t) = \omega v(\omega t)$ and considering the origin as the desired equilibrium point q_e, equation (18) is satisfied for any choice of μ_{11}. Moreover, the equilibrium may be unstable for some values of μ_{11} and stable for other values. We focus on those cases where $h(q_e) \neq 0$ and, as mentioned above, we consider stability separately.

Recalling, from equations (6) to (8), that the parameter μ_{11} is defined solely by the input waveform, it is evident that there are an infinite number of T-periodic, zero-mean functions $v_1(t)$ that satisfy equation (19). Figure 2 shows three such functions: square, sine, and triangular waves, with $T = 1$ and $\mu_{11} = 1$. The square function generates the same input parameter $\mu_{11} = 1$, but with smaller amplitude compared with the other two functions. In the following two theorems it is shown that, of all waveforms generating a given value of μ, the square wave has the smallest amplitude.

Theorem 6. *For any T-periodic, zero-mean function $v(t)$, there exists a phase $0 \le \phi_0 \le T$ such that, for the function $w(t) = v(t + \phi_0)$*

$$\kappa_s = \frac{1}{T}\int_0^T \int_0^t w(\tau)\mathrm{d}\tau\,\mathrm{d}t = 0$$

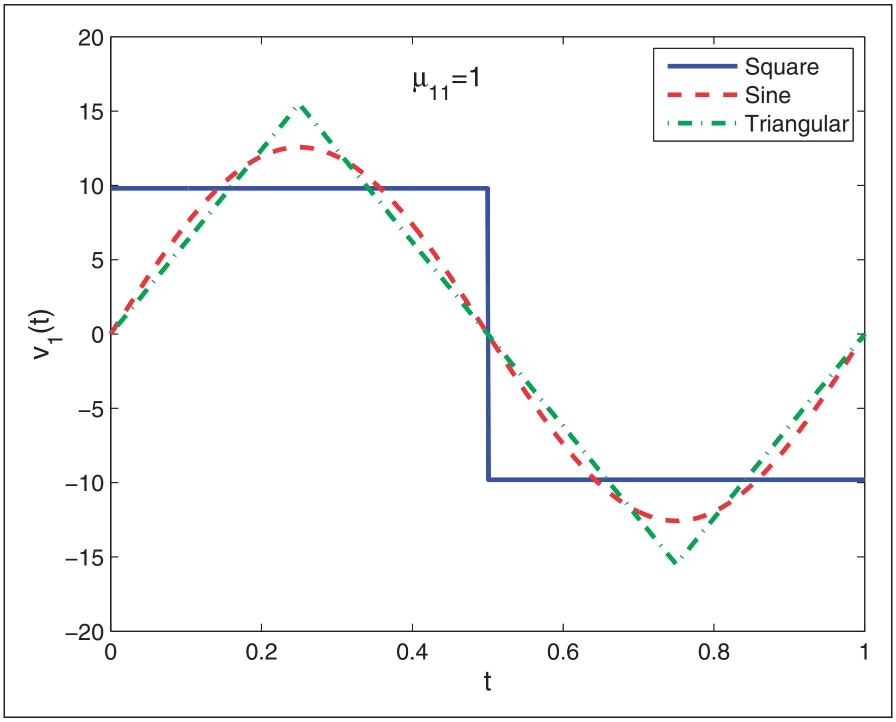

Figure 2. Periodic, zero-mean functions for which $\mu_{11} = 1$.

Proof. See Appendix 1.

Let μ_s represent the value of μ given in equation (8) for the signal $w(t)$. Then according to Theorem 3, μ_s remains constant as ϕ_0 is varied.

Theorem 7. *Of all T-periodic, zero-mean functions $v(t)$ with the same amplitude B, the T-periodic square function*

$$S_B(t) = \begin{cases} B; & 0 \le t \le \dfrac{T}{2} \\ -B; & \dfrac{T}{2} < t \le T \end{cases}$$

results in the largest value μ, as determined using equation (8).

Proof. According to Theorem 6, all T-periodic, zero-mean functions $v(t)$ with the same amplitude B can be shifted by an amount $0 \le \phi \le T$ to make $\kappa_s = 0$, where κ_s is determined using equation (6) for the phase-shifted function, without affecting the value of μ. That is, $\mu = \mu_s = \frac{1}{2}\lambda_s$. (Note that the amount of phase shift ϕ required to make $\kappa_s = 0$ depends on the particular choice of function $v(t)$.) Rather than consider each function $v(t)$ and compare the parameters μ, one may consider the phase-shifted functions $w(t) = v(t + \phi)$ and compare their parameters λ_s; see equation (8). Defining $A_s(t) = \int_0^t w(\tau)d\tau$, and using equation (7), one may write

$$\lambda_s = \int_0^T A_s^2(t)dt$$

The magnitude of the zero-mean square function $S_B(t)$ is maximum for all $t \in \mathbb{R}$, except at isolated times. Thus, for all T-periodic, zero-mean functions $v(t)$ with the same amplitude B, the square function $S_B(t)$ has the maximum absolute area $A(t)$ under the curve t-$v(t)$ for any $t \in [0, T]$, and so has maximum $A_s^2(t)$. Therefore, of all functions $v(t)$ with equal amplitude, the square function $S_B(t)$ has the maximum λ^s, and therefore has the maximum $\mu^s = \mu$. □

Corollary 8. *Of all T-periodic, zero-mean functions with equal values of μ determined using equation* (8), *the T-periodic square function $S_B(t)$ has the minimum amplitude B.*

For function $S_B(t)$ with period T and amplitude B, $\mu = \mu_{\text{square}} = \frac{T^2B^2}{96}$. For any other T-periodic, zero-mean function with an amplitude of B, $\mu < \mu_{\text{square}}$. Note that in equation (4) if the amplitude of the input $v_i(t)$ is B, the total amplitude of the input $u_i(t)$ is ω B.

Remark 9. *As mentioned earlier, this minimum-amplitude input certainly does not ensure stability.*

Analysis may suggest that feedback stabilization is required. Feedback would generally be required, in any case, in order to modulate the system's average motion. See (Tahmasian and Woolsey, 2015), *for example.*

4. Input optimization for multi-input systems

Consider the n-DOF ($n>1$) control-affine system in equation (5). The goal is to determine inputs $v_i(t)$, $i\in\{1,\ldots,m\}$, with amplitudes B_i, for the system to have a periodic orbit in an $O(\epsilon)$ neighborhood of a point $\boldsymbol{x}_e=(\boldsymbol{q}_e^T,\ \boldsymbol{0}_{1\times n})^T$ while minimizing the cost function $J=\sum_{i=1}^m B_i^2$. For the system in equation (5) to have a periodic orbit around point $\boldsymbol{x}_e$, we require that $\boldsymbol{x}_e$ be an equilibrium point of the averaged dynamics in equation (10). Therefore $\boldsymbol{x}_e$ must satisfy

$$\boldsymbol{Z}(\boldsymbol{x}_e)-\sum_{i,j=1}^{m}\mu_{ij}\langle\boldsymbol{Y}_i:\boldsymbol{Y}_j\rangle(\boldsymbol{x}_e)=\boldsymbol{0}_{2n\times1} \tag{20}$$

Since the velocities are identically zero at an equilibrium point and the first n components of the symmetric product are also zero, the first n of the $2n$ algebraic equations (20) are satisfied. The last n equations of equation (17) can be written as

$$\sum_{i,j=1}^{m}\mu_{ij}\boldsymbol{h}_{ij}(\boldsymbol{q}_e)-\boldsymbol{f}(\boldsymbol{q}_e,\boldsymbol{0})=\boldsymbol{0}_{n\times1} \tag{21}$$

where $\boldsymbol{h}_{ij}(\boldsymbol{q}_e)$ is the $n\times1$ vector of the last n components of the symmetric product $\langle\boldsymbol{Y}_i:\ \boldsymbol{Y}_j\rangle(\boldsymbol{x}_e)$. Since $\mu_{ij}=\mu_{ji}$, $i,j\in\{1,\ldots,m\}$, the set of equations (21) consists of n algebraic equations in the $\frac{m(m+1)}{2}$ unknowns μ_{ij}, with $i\le j$. Each of the parameters μ_{ii} depends on the waveform and amplitude of the input $v_i(t)$ and is independent of the others, yielding m unknowns. But the parameters μ_{ij} for $i<j$ depend also on the relative phase between $v_i(t)$ and $v_j(t)$.

The relative phases of the inputs are not all independent. In general, if the phases of all the inputs $v_i(t)$, $i\in\{2,\ldots,m\}$, relative to $v_1(t)$ are known, then the relative phase of any two inputs $v_i(t)$ and $v_j(t)$, $i,j\in\{2,\ldots,m\}$, is also known. Thus there are only $m-1$ independent parameters μ_{ij}, with $i<j$, to be determined from equation (21). In total there are $2m-1$ independent parameters μ_{ij} to be determined. We assume that equation (21) represents a consistent system of algebraic equations and that $2m-1>n$ so that the parameters μ_{ij} are underdetermined.

From the definition of the symmetric product in equation (9) it is evident that $\boldsymbol{h}_{ij}=\boldsymbol{h}_{ji}$. Also from the structure of the class of systems defined by equation (3), the vector fields of the symmetric products $\langle\boldsymbol{Y}_i:\ \boldsymbol{Y}_j\rangle$ are only functions of the generalized coordinates $\boldsymbol{q}$ (and not the velocities $\dot{\boldsymbol{q}}$). Defining

$$\boldsymbol{a}_{ij}=\begin{cases}\boldsymbol{h}_{ij}(\boldsymbol{q}_e) & i=j\\ 2\boldsymbol{h}_{ij}(\boldsymbol{q}_e) & i\neq j\end{cases}$$

and $\boldsymbol{b}=-\boldsymbol{f}(\boldsymbol{q}_e,\boldsymbol{0})$, the set of equations (21) can be written in the form

$$\sum_{i,j=1(i\le j)}^{m}\boldsymbol{a}_{ij}\mu_{ij}+\boldsymbol{b}=\boldsymbol{0} \tag{22}$$

Suppose that μ_{ij}^* denotes a set of solutions of equation (22) where $i,j\in\{1,\ldots,m\}$. Consider a set of T-periodic, zero-mean functions $v_i(t)$ that generate these parameter values $\mu_{ij}=\mu_{ij}^*$. I.e. defining $A_i(t)=\int_0^t v_i(\tau)\mathrm{d}\tau$ assume that

$$\frac{1}{2}\left(\frac{1}{T}\int_0^T A_i^2(t)\mathrm{d}t-\left(\frac{1}{T}\int_0^T A_i(t)\mathrm{d}t\right)^2\right)=\mu_{ii}^*,\quad i\in\{1,\ldots,m\}$$

and

$$\frac{1}{2}\left(\frac{1}{T}\int_0^T A_i(t)A_j(t)\mathrm{d}t-\left(\frac{1}{T}\int_0^T A_i(t)\mathrm{d}t\right)\left(\frac{1}{T}\int_0^T A_j(t)\mathrm{d}t\right)\right)=\mu_{ij}^*,\quad i,j\in\{1,\ldots,m\},\ i<j$$

According to Theorem 7, if one chooses $v_i(t)$ as the T-periodic, zero-mean square function $S_{B_i}(t)$ with an amplitude of $B_i=\frac{4\sqrt{6\mu_{ii}^*}}{T}$, then the amplitude B_i is no greater than the amplitude of any other T-periodic, zero-mean function $v_i(t)$ that generates the same averaged dynamics.

Square wave inputs are appealing for another reason, as well. Note that the parameters μ_{ij} scale the effect of the various symmetric product vector fields in equation (20). Thus, freedom available in choosing a parameter value μ_{ij} enables one to generate time-averaged inputs in the direction defined by the corresponding symmetric product.

Theorem 10. *For all T-periodic, zero-mean functions* $v_1(t)$ *and* $v_2(t)$ *generating certain parameter values* $\mu_{11}\ge0$ *and* $\mu_{22}\ge0$

1. $|\mu_{12}|\le\sqrt{\mu_{11}\mu_{22}}$
2. Choosing the inputs as square functions allows the greatest range of values for μ_{12}, obtained by changing the relative phase of the inputs.

Proof. See Appendix 1.

The input optimization goal presented at the beginning of this section can be restated: Minimize $J = \sum_{i=1}^{m} B_i^2$ under n constraints in equation (22). Thus, one obtains a constrained optimization problem (Bertsekas, 1982; Burns, 2014). The problem may be solved using the method of Lagrange multipliers, redefining the cost function as

$$\psi = \sum_{i=1}^{m} B_i^2 + \sum_{k=1}^{n} \zeta_k \left(\sum_{i,j=1(i \leq j)}^{m} a_{ij_k} \mu_{ij} + b_k \right) \tag{23}$$

where a_{ij_k} and b_k are the kth elements of the vectors $\boldsymbol{a}_{ij}$, and $\boldsymbol{b}$ respectively, and ζ_k, $k \in \{1, \ldots, n\}$, are the Lagrange multipliers.

Using Theorems 7 and 10 it is evident that choosing all the inputs as square functions has two advantages. First, it results in using inputs with smallest amplitudes, and second, it provides the biggest possible range for μ_{ij}, with $i < j$, which can be adjusted by shifting the phases of the various inputs relative to each other. Therefore we choose the inputs as square functions with amplitudes B_i, and seek the relative phases that minimize $\sum_{i=1}^{m} B_i^2$.

The cost function ψ in equation (23) may be rewritten as

$$\psi = \sum_{i=1}^{m} B_i^2 + \sum_{k=1}^{n} \zeta_k \left(\sum_{i=1}^{m} a_{ii_k} \mu_{ii} \right) + \sum_{k=1}^{n} \zeta_k \left(\sum_{i,j=1(i<j)}^{m} a_{ij_k} \mu_{ij} + b_k \right) \tag{24}$$

Since for a T-periodic square function with an amplitude of B_i, we have $\mu_{ii} = \frac{T^2}{96} B_i^2$, the cost function in equation (24) may be expressed as

$$\psi = \sum_{i=1}^{m} \left(1 + \sum_{k=1}^{n} c_{i_k} \zeta_k \right) B_i^2 + \sum_{k=1}^{n} \zeta_k \left(\sum_{i,j=1(i<j)}^{m} a_{ij_k} \mu_{ij} + b_k \right) \tag{25}$$

where $c_{i_k} = \frac{T^2}{96} a_{ii_k}$ and $|\mu_{ij}| \leq \frac{T^2}{96} |B_i B_j|$, with $i < j$.

As mentioned earlier, the parameters μ_{ij}, with $i < j$, are not all independent. To eliminate redundant parameters, one may introduce the relative phase of the inputs. Suppose that the phase of each input $v_i(t)$ relative to $v_1(t)$ is ϕ_i (with $\phi_1 = 0$). Then the relative phase of $v_j(t)$ and $v_i(t)$ is $\phi_{ij} = \phi_j - \phi_i$. For two T-periodic square functions $v_i(t)$ and $v_j(t)$ with amplitudes B_i and B_j, respectively, and a relative phase $\phi_{ij} \in [0, \frac{T}{2}]$, it can be shown that

$$\mu_{ij} = \frac{T^2 B_i B_j}{96} (32\phi_{ij}^3 - 24\phi_{ij}^2 + 1) \tag{26}$$

Therefore, the cost function ψ may be written in terms of $n + 2m - 1$ independent amplitudes B_i, $i \in \{1, \ldots, m\}$, relative phases ϕ_j, $j \in \{2, \ldots, m\}$, and Lagrange multipliers ζ_k, $k \in \{1, \ldots, n\}$ as

$$\begin{aligned}\psi = &\sum_{i=1}^{m} \left(1 + \sum_{k=1}^{n} c_{i_k} \zeta_k \right) B_i^2 \\ &+ \sum_{k=1}^{n} \zeta_k \Bigg(\sum_{i,j=1(i<j)}^{m} \frac{T^2}{96} a_{ij_k} B_i B_j \big(32(\phi_j - \phi_i)^3 \\ &\quad - 24(\phi_j - \phi_i)^2 + 1 \big) + b_k \Bigg)\end{aligned} \tag{27}$$

The extrema of the cost function are its stationary points, which may be found by solving the $n + 2m - 1$ algebraic equations

$$\begin{cases} \dfrac{\partial \psi}{\partial B_i} = 0, & i \in \{1, \ldots, m\} \\ \dfrac{\partial \psi}{\partial \phi_i} = 0, & i \in \{2, \ldots, m\} \\ \dfrac{\partial \psi}{\partial \zeta_k} = 0, & k \in \{1, \ldots, n\} \end{cases} \tag{28}$$

Note that, since $\phi_i \in [0, \frac{T}{2}]$, $i \in \{1, \ldots, m\}$, the set of equations (28) may not have a solution inside the boundaries of ϕ_i, or the solutions may be local extrema. To find the global extrema one should also look for possible solutions on the boundaries of ϕ_i.

As mentioned in Remark 9, an optimal input obtained using this approach is not guaranteed to produce a stable equilibrium. To enforce stability in the optimization process, one could impose additional inequality constraints on the characteristic values of the linearized, time-averaged dynamics. Alternatively, one could defer stability analysis until after the optimal inputs are obtained. If analysis indicates that the resulting equilibrium is unstable but stabilizable, one could design and implement a suitable feedback control strategy after the fact, modulating the input amplitudes, for example, in response to error measurements.

Example 2. Consider the 3-DOF system with three inputs

$$\begin{aligned}\ddot{q}_1 = &-0.5\dot{q}_1^2 + \dot{q}_2^2 + 0.5\dot{q}_3^2 - 2\dot{q}_1\dot{q}_2 - 2.5\dot{q}_1\dot{q}_3 + 0.5\dot{q}_2\dot{q}_3 \\ &- 3.5\dot{q}_1 - \dot{q}_2 + \dot{q}_3 - 5q_1 - 0.02 \\ &+ (q_1 + q_2 + q_3 - 1)u_1(t) \\ \ddot{q}_2 = &\ 1.5\dot{q}_1^2 + 1.5\dot{q}_3^2 - 0.5\dot{q}_1\dot{q}_2 - 1.5\dot{q}_1\dot{q}_3 - 2\dot{q}_2\dot{q}_3 + \dot{q}_1 \\ &- 3.5\dot{q}_2 + \dot{q}_3 - 5q_2 - 0.3 \\ &+ (q_1 - q_2 + q_3 - 1)u_2(t)\end{aligned}$$

$$\ddot{q}_3 = \dot{q}_1^2 + 0.5\dot{q}_2^2 + 1.5\dot{q}_3^2 - 0.5\dot{q}_1\dot{q}_2 + 1.5\dot{q}_1\dot{q}_3 + 0.5\dot{q}_2\dot{q}_3 - \dot{q}_1 - 4.5\dot{q}_3 - 5q_3 - 0.15 + (q_1 + q_2 + 2q_3 + 1)u_3(t) \quad (29)$$

where $u_i(t) = \omega v_i(\omega t + \phi_i)$, $i \in \{1, 2, 3\}$, are high-frequency, high-amplitude periodic inputs. The goal is for the system to have a periodic orbit in an $O(\epsilon)$ neighborhood of the origin, where $\epsilon = \frac{1}{\omega}$, when using inputs with the minimum possible amplitudes.

Considering $v_i(t)$, $i \in \{1, 2, 3\}$, as T-periodic, square functions with amplitudes B_i and using Theorem 1, the averaged dynamics of equation (29) can be determined. The averaged equations are not shown here. For the original system to have a periodic orbit around the origin, we require that the origin be an equilibrium point of the averaged system. Setting the state to zero in the averaged dynamics, the three constraint equations are

$$\begin{cases} B_1^2 + 2B_2^2 + B_3^2 - 64\Delta_{22}B_1B_2 + 96\Delta_{33}B_1B_3 \\ \quad -\Delta_{23}B_2B_3 - 1.92 = 0 \\ 3B_1^2 - 2B_2^2 + 3B_3^2 + 32\Delta_{22}B_1B_2 + 96\Delta_{33}B_1B_3 \\ \quad +2\Delta_{23}B_2B_3 - 28.8 = 0 \\ 2B_1^2 + B_2^2 - B_3^2 - 32\Delta_{22}B_1B_2 - 32\Delta_{33}B_1B_3 \\ \quad +\Delta_{23}B_2B_3 - 14.4 = 0 \end{cases} \quad (30)$$

where

$$\Delta_{22} = (\phi_2 - 0.68)(\phi_2 - 0.25)(\phi_2 + 0.18)$$

$$\Delta_{33} = (\phi_3 - 0.68)(\phi_3 - 0.25)(\phi_3 + 0.18)$$

and

$$\Delta_{23} = 1 - 24(\phi_2 - \phi_3)^2 - 32(\phi_2 - \phi_3)^3$$

Using the constraint equations (30), the cost function ψ can be determined from equation (27). Now one may use mathematical software or numerical methods to find the global minimum of the cost function when $0 \le \phi_i \le \frac{T}{2}$, $i \in \{2,3\}$. Also, one must check the stability of the origin for the optimum solution. For this example, using both Mathematica and Matlab, and using $T = 1$, the optimum solution was determined as $B_1 = 2.876$, $B_2 = 0.675$, $B_3 = 1.88$, $\phi_2 = 0.09$, and $\phi_3 = 0.33$. Using the linearization of the averaged dynamics about the origin, for these optimum values the origin is a stable equilibrium point for the averaged dynamics. The simulation results of the original and averaged dynamics using the optimum inputs are shown in Figure 3. The initial conditions of the simulations are $\boldsymbol{x}(0) = (0.2, 0.2, -0.2, 0, 0, 0)^T$ and the frequency $\omega = 3\pi$. Note that the initial conditions of the averaged dynamics are different (in this case $\bar{\boldsymbol{x}}(0) = (0.2, 0.2, -0.2, -0.575, -0.131, -0.15)^{\mathrm{T}}$).

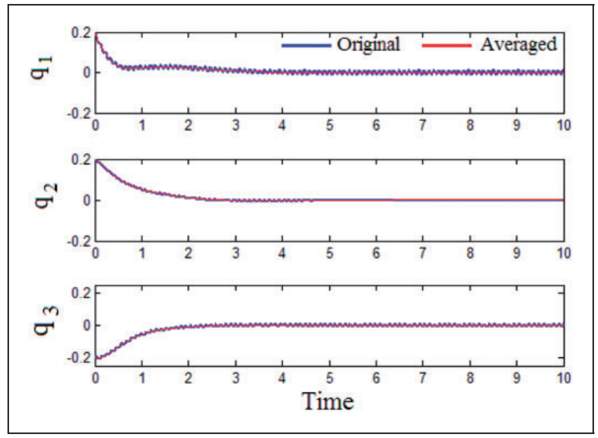

Figure 3. Time histories of the original system in equation (29) and the averaged system when using the optimum inputs.

5. Alternate description of input waveforms

Instead of choosing a particular shape for the input waveforms and adjusting the amplitude and phase, a general class of input waveforms can be defined using a finite Fourier series. This formulation is similar to the method for constructing periodic inputs by summing sinusoids at different frequencies presented in (Vela, 2003; Vela et al., 2002a,b). Consider the finite Fourier series of the zero-mean, T-periodic input waveform $v_i(t)$

$$v_i(t) = \sum_{n=1}^{l} \big(A_{i,n}\cos(\Omega nt) + B_{i,n}\sin(\Omega nt)\big) \quad (31)$$

where $A_{i,n}$, $B_{i,n}$ are Fourier coefficients and $\Omega = 2\pi/T$, where T is the base period. For convenience we define $a_{i,n} = A_{i,n}/\Omega$ and $b_{i,n} = B_{i,n}/\Omega$, and rewrite the finite Fourier series equation (31) in the form of

$$v_i(t) = \Omega \sum_{n=1}^{l} \big(a_{i,n}\cos(\Omega nt) + b_{i,n}\sin(\Omega nt)\big) \quad (32)$$

The Fourier coefficients $a_{i,n}$ and $b_{i,n}$ are treated as free parameters.

Theorem 11. *If the input waveforms $v_i(t)$ and $v_j(t)$ are expressed in the form of equation* (32), *the parameters κ_i* and μ_{ij} are

$$\kappa_i = \sum_{n=1}^{l} \frac{b_{i,n}}{n} \quad \text{and} \quad \mu_{ij} = \frac{1}{4}\sum_{n=1}^{l}\left(\frac{1}{n^2}\left(a_{i,n}a_{j,n} + b_{i,n}b_{j,n}\right)\right)$$

Proof. See Appendix 1.

To introduce a notion of amplitude that is consistent with earlier discussions of the input waveform, we make the following definition.

Definition 12. *The amplitude of a zero-mean, T-periodic function w(t) is*

$$\mathbf{amp}\, w = \frac{1}{2}\left(\max_{t\in[0,T]} w - \min_{t\in[0,T]} w\right)$$

Once again we formulate a constrained optimization problem with the cost functional $J = \sum_{i=1}^{m}(\mathbf{amp}\, v_i(t))^2$ subject to the constraint in equation (22). Since the input waveforms are defined using finite Fourier series, the decision variables are the Fourier coefficients.

Since the value of μ_{ij} only depends on the relative phase between inputs, if the phase of all of the inputs is shifted equally, the values of all μ_{ij} will remain constant. Therefore, any phase shift $\phi \in [0, 2\pi]$ that is applied uniformly to the trigonometric terms in equation (32) will result in input waveforms that satisfy the constraints with the same value of the cost functional. Thus, there are infinitely many locally optimal input waveforms, each with the same cost. The primary problem this poses is that it becomes impractical to find the optimum waveforms using the Lagrange multiplier method described previously. Instead, a numerical optimization technique is used.

Example 3. Consider the planar two-link mechanism on a cart depicted in Figure 4. Each link is a uniform bar with mass m_i, $i \in \{1, 2\}$, length l_i, and mass moment of inertia $I_i = \frac{1}{12}m_i l_i^2$ about its center of mass. The mass of the cart is m_c. The system is a 3-DOF system with two inputs and moves in a horizontal plane; gravity does not affect the motion. The inputs are the force $F(t)$ acting on the cart and the torque $\tau(t)$ acting on the first link. We assume the system is subject to linear damping with coefficients of k_{d_1} and k_{d_2} in the first and second joints, respectively. Considering $\boldsymbol{q} = (x, \theta_1, \theta_2)^T$ as the vector of generalized coordinates, the goal is to generate a stable periodic orbit in a $O(\epsilon)$ neighborhood of a desired configuration $\boldsymbol{q}_d = (x_d, \theta_{d_1}, \theta_{d_2})^{\mathrm{T}}$, while using inputs with minimum amplitudes. The dynamic equations of the system can be written in the form

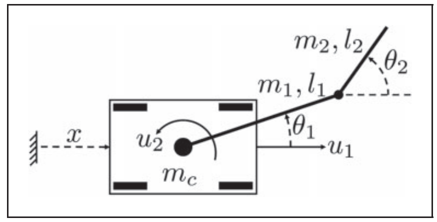

Figure 4. Two-link mechanism on a cart.

$$\boldsymbol{M}(\boldsymbol{q})\ddot{\boldsymbol{q}} = \boldsymbol{f}(\boldsymbol{q}, \dot{\boldsymbol{q}}) + \boldsymbol{F}_{\mathrm{c}}(t)$$

where the generalized inertia matrix is

$$\boldsymbol{M}(\boldsymbol{q}) = \begin{pmatrix} m_c + m_1 + m_2 & -\frac{1}{2}(m_1 + 2m_2)l_1 \sin\theta_1 & -\frac{1}{2}m_2 l_2 \sin\theta_2 \\ -\frac{1}{2}(m_1 + 2m_2)l_1 \sin\theta_1 & I_1 + \frac{1}{4}(m_1 + 4m_2)l_1^2 & \frac{1}{2}m_2 l_1 l_2 \cos(\theta_1 - \theta_2) \\ -\frac{1}{2}m_2 l_2 \sin\theta_2 & \frac{1}{2}m_2 l_1 l_2 \cos(\theta_1 - \theta_2) & I_2 + \frac{1}{4}m_2 l_2^2 \end{pmatrix}$$

and

$$\boldsymbol{f}(\boldsymbol{q}, \dot{\boldsymbol{q}}) = \begin{pmatrix} \frac{1}{2}\left((m_1 + 2m_2)l_1\dot{\theta}_1^2 \cos\theta_1 + m_2 l_2 \dot{\theta}_2^2 \cos\theta_2\right) \\ -\frac{1}{2}m_2 l_1 l_2 \dot{\theta}_2^2 \sin(\theta_1 - \theta_2) - k_{d_1}\dot{\theta}_1 + k_{d_2}(\dot{\theta}_2 - \dot{\theta}_1) \\ \frac{1}{2}m_2 l_1 l_2 \dot{\theta}_1^2 \sin(\theta_1 - \theta_2) - k_{d_2}(\dot{\theta}_2 - \dot{\theta}_1) \end{pmatrix}$$

and the vector of inputs is

$$\boldsymbol{F}_{\mathrm{c}}(t) = \begin{pmatrix} F(t) \\ \tau(t) \\ 0 \end{pmatrix}$$

Consider the following inputs

$$\begin{aligned} F(t) &= -k_{\mathrm{p_c}}(x - x_d) - k_{\mathrm{d_c}}\dot{x} + \omega v_1(\omega t) \\ \tau(t) &= \tau_{\mathrm{s}} - k_{p_1}(\theta_1 - \theta_{d_1}) + \omega v_2(\omega t + \phi) \end{aligned} \tag{33}$$

where $v_1(t)$ and $v_2(t)$ are T-periodic, zero-mean functions with amplitudes of F_0 and τ_0 respectively, $k_{\mathrm{p_c}}$, k_{p_1}, and $k_{\mathrm{d_c}}$ are control parameters, and τ_s is a nonzero constant.

Using the state vector $\boldsymbol{x} = (\boldsymbol{q}^{\mathrm{T}}, \dot{\boldsymbol{q}}^{\mathrm{T}})^{\mathrm{T}}$, one may transform the equations of motion of the system into the form of equation (5) with $m = 2$, and determine the averaged dynamics using Theorem 1. The averaged dynamics are in the form

$$\dot{\bar{x}} = Z(\bar{x}) - \sum_{i,j=1}^{2} \mu_{ij}\langle Y_i : Y_j\rangle(\bar{x}) \tag{34}$$

where

$$Y_i(x) = \begin{pmatrix} \mathbf{0}_{3\times 1} \\ M_i^{-1}(q) \end{pmatrix}$$

with $M_i^{-1}(q)$ being the ith column of $M^{-1}(q)$, and

$$Z(x) = \begin{pmatrix} \dot{q} \\ M^{-1}(q)\big(f(q,\dot{q}) + g(q,\dot{q})\big) \end{pmatrix}$$

where

$$g(q,\dot{q}) = \begin{pmatrix} -k_{\mathrm{p_c}}(x - x_d) - k_{\mathrm{d_c}}\dot{x} \\ \tau_s - k_{p_1}(\theta_1 - \theta_{d_1}) \\ 0 \end{pmatrix}$$

Using the inputs in equation (33), the system may possess a stable periodic orbit in an $O(\frac{1}{\omega})$ neighborhood of q_d. This happens if the point $x_{\mathrm{e}} = (q_d^{\mathrm{T}}, \mathbf{0}_{1\times 3})^{\mathrm{T}}$ is a hyperbolically stable equilibrium point of the averaged dynamics. For the point x_e to be an equilibrium point of the averaged system, it must satisfy

$$Z(x_{\mathrm{e}}) - \sum_{i,j=1}^{2} \mu_{ij}\langle Y_i : Y_j\rangle(x_{\mathrm{e}}) = \mathbf{0} \tag{35}$$

The set of algebraic equations (35) contains six equations, the first three being satisfied automatically because of the system structure. For the point q_d to be an equilibrium point of the averaged dynamics, one needs to choose parameters to satisfy the last three equations of equation (35).

To establish a periodic orbit about the point q_d one should choose a value for τ_s and find μ_{ij}, $i,j \in \{1,2\}$, to satisfy the equations in equation (35). Depending on the physical parameters of the system, there may be no acceptable solution for τ_s and μ_{ij}. As mentioned earlier, however, in the discussion following equation (21), we assume that equation (35) represents a consistent set of algebraic equations.

Only two of the last three equations of equation (35) are independent. Therefore there is a set of two independent equations in three unknowns $\mu_{ij} = \mu_{ji}$. The equations yield a one-parameter family of solutions. There is thus parametric freedom available for further optimization.

Consider the case where the links have mass per unit length ρ_m. For the physical parameters

$$\begin{aligned} &m_{\mathrm{c}} = 1\ \mathrm{kg}, \quad \rho_m = 1\ \mathrm{kg/m}, \quad l_1 = 0.8\ \mathrm{m}, \quad l_2 = 1\ \mathrm{m} \\ &k_{\mathrm{p_c}} = 5, \quad k_{\mathrm{d_c}} = 2, \quad k_{p_1} = 10, \quad k_{d_1} = 2, \quad k_{d_2} = 1 \end{aligned}$$

and for $x_{\mathrm{d}} = 0$, $\theta_{d_1} = -\frac{\pi}{9}$ rad, $\theta_{d_2} = \frac{\pi}{9}$ rad, and $\tau_s = 1$ N·m, the set of equations (35) to be satisfied are

$$\begin{aligned} 0.2271\mu_{11} - 0.6111\mu_{12} - 1.5465\mu_{22} &= -0.4727 \\ 1.0179\mu_{11} - 3.1218\mu_{12} - 5.9772\mu_{22} &= -2.3732 \\ 1.4390\mu_{11} - 3.0137\mu_{12} - 11.9323\mu_{22} &= -2.4241 \end{aligned} \tag{36}$$

The set of equations (36) contains two independent equations in three unknowns and there are infinitely many inputs $v_1(t)$ and $v_2(t)$ to be chosen. Choosing $F_0^2 + \tau_0^2$ as the cost function to be minimized, according to Theorem 7 one should choose the inputs as T-periodic, zero-mean square functions with amplitudes F_0 and τ_0 and a relative phase ϕ, to be determined using the optimization procedure discussed in Section 4. Considering square inputs with $T = 2\pi$ s, one determines $F_0 = 4.336$ N, $\tau_0 = 1.202$ N·m, and $\phi = 0$ as the optimal inputs.

The input waveform optimization problem for this system was also solved using the alternate method described in Section 5. The input waveforms $v_1(t)$ and $v_2(t)$ are described as finite Fourier series and $(\mathbf{amp}, v_1(t))^2 + (\mathbf{amp}, v_2(t))^2$ is chosen as the cost functional. The results of this technique, along with a comparison to the previous technique, are shown in Figure 5. As can be seen, the results from the finite Fourier series technique approach the square wave as the number of Fourier coefficients increases.

The averaged system is then linearized about the desired equilibrium point x_e, and control parameters are sought to stabilize the resulting linear system. Figure 6 shows simulation results using the optimum inputs with $\omega = 50$ rad/s. In this simulation, the initial velocity is zero and the initial configuration is $x_0 = 0.2$ m, $\theta_{1_0} = \frac{\pi}{6}$ rad, $\theta_{2_0} = \frac{\pi}{3}$ rad.

As stated in Theorem 7, a square wave is the optimal solution for the cost functional $J = \sum_{i=1}^{m}(\mathbf{amp}\, v_i(t))^2$. However if a different cost functional is chosen, the square wave will not be the optimal input waveform, in general, and the finite Fourier series may yield superior results.

6. Input energy minimization

Minimizing the sum of the square of the amplitudes of the input waveforms is a well-motivated cost functional, because the input amplitude relates to actuator

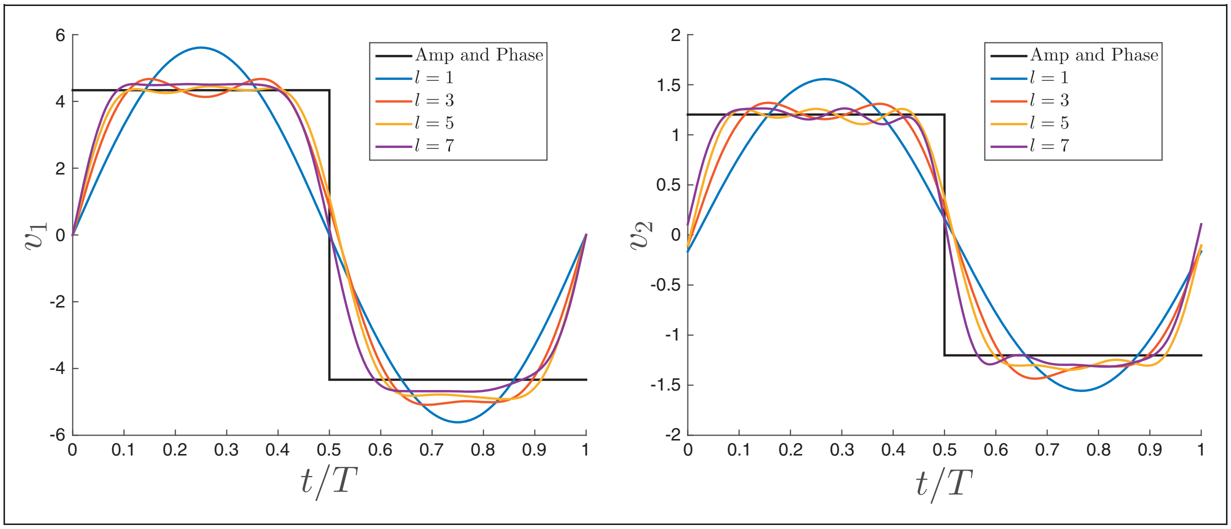

Figure 5. Optimal input waveforms for the cart with two-link mechanism obtained using the approaches described in Section 4 and Section 5. The different solutions for the finite Fourier series correspond to different numbers of Fourier coefficients $l \in \{1, 3, 5, 7\}$.

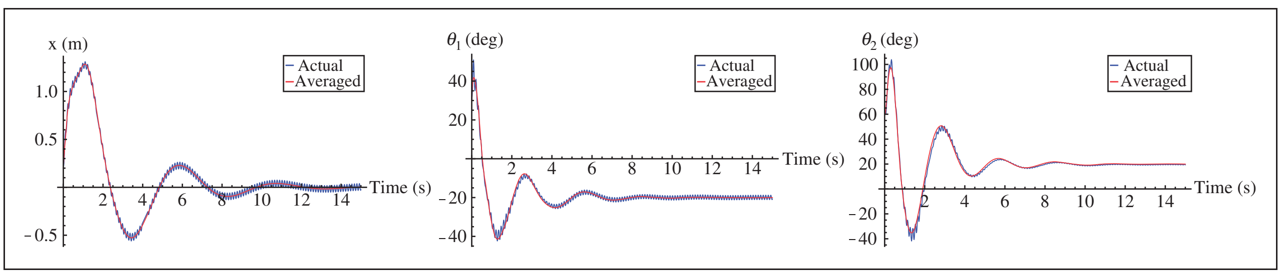

Figure 6. Time histories of $x(t)$, $\theta_1(t)$, and $\theta_2(t)$ of the two-link mechanism on a cart.

sizing requirements. Another well-motivated optimization objective is minimizing the input energy. Suppose $\boldsymbol{u}(t)$ is an input history that drives a system, $\dot{\boldsymbol{x}} = \boldsymbol{f}(t, \boldsymbol{x}(t), \boldsymbol{u}(t))$, from $\boldsymbol{x}_0$ at time $t=0$ to $\boldsymbol{x}_f$ at time $t=t_f$. The input energy is defined as (Burns, 2014)

$$E(t_f) = \frac{1}{2}\int_0^{t_f} \boldsymbol{u}^{\mathrm{T}}(t)\boldsymbol{u}(t)\mathrm{d}t \tag{37}$$

If the inputs are T-periodic and $t_f = kT$ for some $k \in \mathbb{Z}^+$, then

$$E(kT) = \frac{k}{2}\int_0^{T} \boldsymbol{u}^{\mathrm{T}}(t)\boldsymbol{u}(t)\mathrm{d}t \tag{38}$$

Defibition 13. *The τ-averaged p-norm of a p-integrable vector signal $\boldsymbol{u}(t)$ is*

$$\|\boldsymbol{u}(t)\|_{\tau,p} = \left(\frac{1}{\tau}\int_0^{\tau} \sum_{i=1}^{m} |u_i(t)|^p \,\mathrm{d}t\right)^{\frac{1}{p}}$$

where $u_i(t)$ is the ith element of $\boldsymbol{u}(t)$.

Using this definition, the T-averaged 2-norm of the T-periodic input history $u(t)$ is equal to

$$\|\boldsymbol{u}(t)\|_{T,2} = \sqrt{\frac{1}{T}\int_0^{T} \boldsymbol{u}^{\mathrm{T}}(t)\boldsymbol{u}(t)\mathrm{d}t}$$

The T-averaged p-norm in Definition 13 satisfies the required properties of a norm (Khalil, 1996).

Proposition 14. *If $v_i(t)$ is defined as a finite Fourier series as in equation* (32), *i.e.*

$$v_i(t) = \Omega \sum_{n=1}^{l} \big(a_{i,n}\cos(\Omega n t) + b_{i,n}\sin(\Omega n t)\big)$$

then the T-averaged 2-norm can be expressed as

$$\|\boldsymbol{v}(t)\|_{T,2} = \sqrt{\frac{1}{T}\int_0^{T} \boldsymbol{v}^{\mathrm{T}}(t)\boldsymbol{v}(t)\mathrm{d}t} = \frac{\Omega}{\sqrt{2}}\sqrt{\sum_{i=1}^{m}\sum_{n=1}^{l}\big(a_{i,n}^2 + b_{i,n}^2\big)}$$

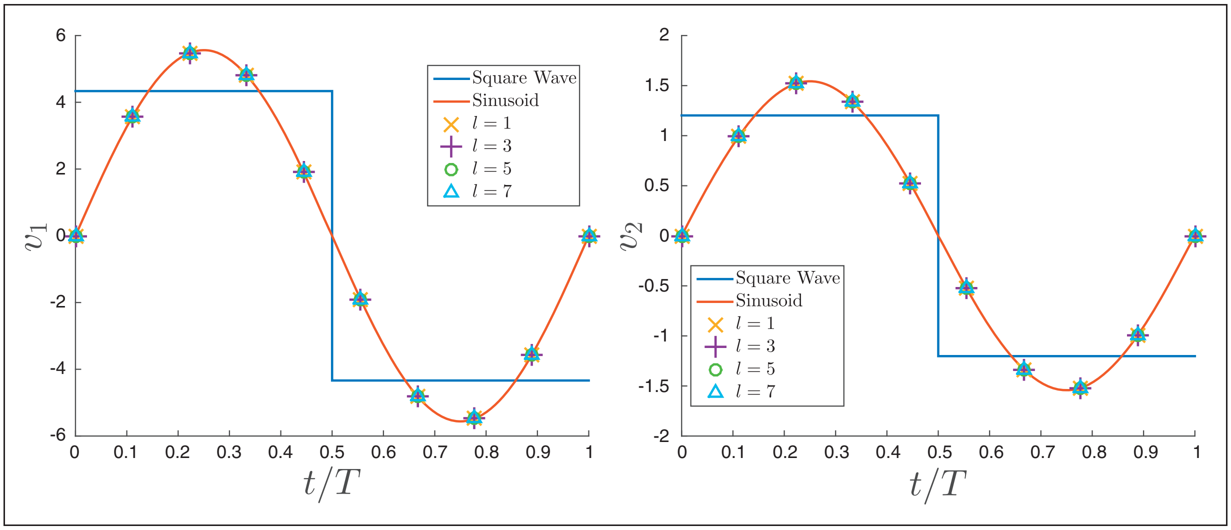

Figure 7. The minimal input energy waveforms for waveforms expressed as square waves, sinusoids, and finite Fourier series with $l \in \{1, 3, 5, 7\}$.

Proof. The proof is straight forward and is omitted.

Remark 15. *Similar to square waves, there exists an expression to easily compute* μ_{ij}*. Considering the input waveforms* $v_i(t) = B_i \cos(\Omega t + \phi_i)$ and $v_j(t) = B_j \cos(\Omega t + \phi_j)$

$$\mu_{ij} = \frac{b_i b_j}{4} \cos(\phi_{ij})$$

where $B_i = b_i \Omega$, *and* $\phi_{ij} = \phi_j - \phi_i$.

Therom 16. *Let* $\mathbf{v}(t) = [v_1(t), \ldots, v_m(t)]^T$ *be a vector of continuous, zero-mean, T-periodic input waveforms satisfying the conditions in equation* (22). *For the corresponding values of* μ_{ij}*, the minimum input energy corresponds to sinusoidal input waveforms, i.e.* $v_i(t) = B_i cos(\Omega t + \phi_i)$.

Proof. See Appendix 1.

Recall that the amplitude cost functional considered earlier was $\sum_{i=1}^{m} (\mathbf{amp}\, v_i(t))^2$. For square waves or sinusoids, this can be written as $\sum_{i=1}^{m} B_i^2$. Notice that the input energy for square waves and sinusoids is proportional to the sum of the square of the amplitudes, i.e. for input waveforms expressed as square waves or sinusoids $\|v(t)\|_{T,2}^2 \propto \sum_{i=1}^{m} B_i^2$. Therefore, if the input waveforms are defined as square waves, the same input waveforms minimize both $\sum_{i=1}^{m} (\mathbf{amp}\, v_i(t))^2$ and $\|v(t)\|_{T,2}^2$, and likewise for input waveforms defined as sinusoids. The proportionality constant is different when considering square waves and sinusoids and this difference leads to Corollary 8 suggesting that square waves are the best choice for minimizing $\sum_{i=1}^{m} (\mathbf{amp}\, v_i(t))^2$ and Theorem 16 suggesting that sinusoids are the best choice for minimizing the input energy.

Example 4. This example concerns the system defined in Example 3. Instead of minimizing the input amplitudes as in Example 3, we minimize the input energy. The results of this optimization problem can be seen in Figure 7. Comparing with Figure 5, the square wave and finite Fourier series with $l = 1$ are the same in both figures, but all of the other input waveforms are different in the figures. This is the result of the fact that both optimization problems are equivalent for square waves and sinusoids, but not for finite Fourier series. The optimal waveforms defined as finite Fourier series are also the same as the optimal sinusoid. This is the expected result; Theorem 16 shows that sinusoids minimize the input energy. Simulations of the system dynamics are qualitatively similar to those of Figure 6.

Remark 17. *The input optimization discussed in this paper may also be used for design optimization of control-affine mechanical systems. The design parameters may include physical system parameters as well as control parameters. The design challenge is to determine the input waveforms and the design parameters* p*, within acceptable ranges, that minimize a given cost function while establishing a desired periodic orbit. If the resulting periodic orbit is unstable, it may be stabilized through feedback control or stability may be enforced through additional constraints in the optimization problem. As discussed in the introduction, additional analysis (e.g. using stability maps, as in* Berg and Wickramasinghe

(2015)) *may be required to ensure that the forcing frequency ω exceeds the critical value*.

7. Conclusion

This paper addresses the input optimization of vibrational control systems. By studying the effects of the input signal waveforms on the averaged dynamics of the vibrational system, we showed that periodic square inputs require smaller amplitudes to effect a given periodic motion than other periodic waveforms. Using the averaged dynamics, the problem of input optimization was transformed into a constrained optimization problem. Solving the constrained optimization problem, one determines the minimum amplitude of each input and the relative phase between them. It was shown that shifting all the inputs by the same amount does not affect the averaged dynamics, as one would expect. However, shifts in the relative phase between input waveforms may alter the character (e.g. the existence or stability of equilibria and periodic orbits). An alternative method of optimizing the input waveforms, using a finite Fourier series to define a general class of inputs was also presented. When using finite Fourier series as the input waveforms, the optimal solution to the input amplitude minimization problem approximates a square wave as the number of terms increases. Finally, a second constrained optimization was presented, with the aim of minimizing the input energy for vibrational control. For this problem, the optimal input waveforms were shown to be sinusoids.

Acknowledgements

The authors gratefully acknowledge the constructive comments of the anonymous reviewers.

Funding

This work was supported by the National Science Foundation (grant number CMMI-1435484).

References

Anderson ML and Cobb RG (2012) Toward flapping wing control of micro air vehicles. *Journal of Guidance, Control, and Dynamics* 35(1): 296–308.

Bellman R, Bentsman J and Meerkov SM (1985) Stability of fast periodic systems. *IEEE Transactions on Automatic Control* AC-30(3): 289–291.

Bellman RE, Bentsman J and Meerkov SM (1986a) Vibrational control of nonlinear systems: Vibrational controllability and transient behavior. *IEEE Transactions on Automatic Control* AC-31(8): 717–724.

Bellman RE, Bentsman J and Meerkov SM (1986b) Vibrational control of nonlinear systems: Vibrational stabilizability. *IEEE Transactions on Automatic Control* AC-31(8): 710–716.

Berg JM and Wickramasinghe IPM (2015) Vibrational control without averaging. *Automatica* 58: 72–81.

Berman GJ and Wang ZJ (2007) Energy-minimizing kinematics in hovering insect flight. *Journal of Fluid Mechanics* 582: 153–168.

Bertsekas DP (1982) *Constrained Optimization and Lagrange Multiplier Methods*. Computer Science and Applied Mathematics. New York, NY: Academic Press.

Bobrow JE, Dubowsky S and Gibson JS (1985) Time-optimal control of robotic manipulators along specified paths. *The International Journal of Robotics Research* 4(3): 3–17.

Bullo F (2002) Averaging and vibrational control of mechanical systems. *SIAM Journal on Control and Optimization* 41(2): 542–562.

Bullo F and Lewis AD (2005) *Geometric Control of Mechanical Systems*. Texts in Applied Mathematics. New York, NY: Springer.

Burns JA (2014) *Introduction to the Calculus of Variations and Control with Modern Applications*. Chapman and Hall/CRC Applied Mathematics and Nonlinear Science. Boca Raton, FL: CRC Press.

Chedmail P and Gautier M (1990) Optimum choice of robot actuators. *ASME Journal of Engineering for Industry* 112: 361–367.

Gregory J, Olivares A and Staffetti E (2012) Energy-optimal trajectory planning for robot manipulators with holonomic constraints. *Systems and Control Letters* 61(2): 279–291.

Guckenheimer J and Holmes P (1983) *Nonlinear Oscillations, Dynamical Systems, and Bifurcations of Vector Fields*. Applied Mathematical Sciences. New York, NY: Springer-Verlag.

Kapitza PL (1965) Dynamical stability of a pendulum when its point of suspension vibrates. In: ter Haar D (ed.) *Collected Papers by P. L. Kapitza*. Vol. 2. Pergamon, pp. 714–725.

Karpelson M, Wei G and Wood RJ (2008) A review of actuation and power electronics options for flapping-wing robotic insects. In: *IEEE International Conference on Robotics and Automation*, Pasadena, California, USA, 19–23 May 2008, pp.779–786.

Khalil HK (1996) *Nonlinear Systems*. Upper Saddle River, NJ: Prentice-Hall, Inc.

Martinez S, Cortes J and Bullo F (2003) Analysis and design of oscillatory control systems. *IEEE Transactions on Automatic Control* 48(7): 1164–1177.

Meerkov SM (1973) Averaging of trajectories of slow dynamic systems. *Differential Equations* 9(9): 1239–1245.

Meerkov SM (1977) Vibrational control theory. *Journal of The Franklin Institute* 303(2): 117–128.

Mitrinovic S, Pecaric JE and Fink AM (1993) *Classical and New Inequalities in Analysis*. Mathematics and its Applications. Dordrecht, The Netherlands: Kluwer Academic Publishers.

Oppenheimer MW, Doman DB and Sigthorsson DO (2011) Dynamics and control of a biomimetic vehicle using biased

wingbeat forcing functions. *Journal of Guidance, Control, and Dynamics* 34(1): 204–217.
Salas SL, Etgen GJ and Hille E (2006) *Calculus: One and Several Variables*. New York, NY: John Wiley and Sons, Inc.
Sanders JA and Verhulst F (1985) *Averaging Methods in Nonlinear Dynamical Systems*. Applied Mathematical Sciences. New York, NY: Springer-Verlag.
Tahmasian S and Woolsey CA (2015) A control design method for underactuated mechanical systems using high frequency inputs. *ASME Journal of Dynamic Systems, Measurement, and Control* 137(7): 071004–11.
Vela PA (2003) *Averaging and Control of Nonlinear Systems (with Application to Biomimetic Locomotion)*. PhD Thesis, California Institute of Technology, Pasadena, CA, USA.
Vela PA, Morgansen KA and Burdick JW (2002a) Second order averaging methods for oscillatory control of underactuated mechanical systems. In: *American Control Conference*, Anchorage, Alaska, USA, 8–10 May 2002, pp.4672–4677.
Vela PA, Morgansen KA and Burdick JW (2002b) Underwater locomotion from oscillatory shape deformations. In: *IEEE Conference on Decision and Control*, Las Vegas, Nevada, USA, 10–13 December 2002, pp.2074–2080.
Wood RJ (2008) The first takeoff of a biologically inspired at-scale robotic insect. *Transactions on Robotics* 24(2): 341–347.

Appendix 1

Proof of Theorem 3. Since $v_i(t)$, $i \in \{1, \dots, m\}$, is a zero-mean, T-periodic function, $w_i(t)$ is also a zero-mean, T-periodic function. For $w_i(t)$ and $w_j(t)$, $i, j \in \{1, \dots, m\}$ we define

$$\kappa_{s_i} = \frac{1}{T}\int_0^T \int_0^t w_i(\tau)\mathrm{d}\tau\,\mathrm{d}t \tag{39}$$

$$\lambda_{s_{ij}} = \frac{1}{T}\int_0^T \left(\int_0^t w_i(\tau)\mathrm{d}\tau\right)\left(\int_0^t w_j(\tau)\mathrm{d}\tau\right)\mathrm{d}t \tag{40}$$

and

$$\mu_{s_{ij}} = \frac{1}{2}(\lambda_{s_{ij}} - \kappa_{s_i}\kappa_{s_j}) \tag{41}$$

Using Theorem 1, the averaged dynamics of equation (11) is

$$\dot{\bar{\boldsymbol{y}}} = \boldsymbol{Z}(\bar{\boldsymbol{y}}) - \sum_{i,j=1}^{m} \mu_{s_{ij}} \langle \boldsymbol{Y}_i : \boldsymbol{Y}_j \rangle(\bar{\boldsymbol{y}})$$

with an initial condition $\bar{\boldsymbol{y}}(0) = \boldsymbol{x}_0 + \sum_{i=1}^m \kappa_{s_i}\boldsymbol{Y}_i(\boldsymbol{x}_0)$.

For any $\phi_0 \in [0, T]$, we show that $\mu_{s_{ij}} = \mu_{ij}$. Using $w_i(t) = v_i(t + \phi_0)$, the parameter $\mu_{s_{ij}}$ can be written as

$$\begin{aligned}\mu_{s_{ij}} &= \frac{1}{2T}\int_0^T \left(\int_0^t v_i(\tau+\phi_0)\mathrm{d}\tau\right)\left(\int_0^t v_j(\tau+\phi_0)\mathrm{d}\tau\right)\mathrm{d}t \\ &\quad - \frac{1}{2T^2}\left(\int_0^T \int_0^t v_i(\tau+\phi_0)\mathrm{d}\tau\,\mathrm{d}t\right) \\ &\quad \times \left(\int_0^T \int_0^t v_j(\tau+\phi_0)\mathrm{d}\tau\,\mathrm{d}t\right)\end{aligned} \tag{42}$$

Using $s = \tau + \phi_0$, equation (42) can be rewritten as

$$\begin{aligned}\mu_{s_{ij}} &= \frac{1}{2T}\int_0^T \left(\int_{\phi_0}^{t+\phi_0} v_i(s)\mathrm{d}s\right)\left(\int_{\phi_0}^{t+\phi_0} v_j(s)\mathrm{d}s\right)\mathrm{d}t \\ &\quad - \frac{1}{2T^2}\left(\int_0^T \int_{\phi_0}^{t+\phi_0} v_i(s)\mathrm{d}s\,\mathrm{d}t\right)\left(\int_0^T \int_{\phi_0}^{t+\phi_0} v_j(s)\mathrm{d}s\,\mathrm{d}t\right)\end{aligned}$$

which can be expanded to

$$\begin{aligned}\mu_{s_{ij}} &= \frac{1}{2T}\int_0^T \left(\int_0^{t+\phi_0} v_i(s)\mathrm{d}s - \int_0^{\phi_0} v_i(s)\mathrm{d}s\right) \\ &\quad \times \left(\int_0^{t+\phi_0} v_j(s)\mathrm{d}s - \int_0^{\phi_0} v_j(s)\mathrm{d}s\right)\mathrm{d}t \\ &\quad - \frac{1}{2T^2}\left(\int_0^T \left(\int_0^{t+\phi_0} v_i(s)\mathrm{d}s - \int_0^{\phi_0} v_i(s)\mathrm{d}s\right)\mathrm{d}t\right) \\ &\quad \times \left(\int_0^T \left(\int_0^{t+\phi_0} v_j(s)\mathrm{d}s - \int_0^{\phi_0} v_j(s)\mathrm{d}s\right)\mathrm{d}t\right)\end{aligned} \tag{43}$$

Equation (43) simplifies to

$$\begin{aligned}\mu_{s_{ij}} &= \frac{1}{2T}\int_0^T \left(\int_0^{t+\phi_0} v_i(s)\mathrm{d}s\right)\left(\int_0^{t+\phi_0} v_j(s)\mathrm{d}s\right)\mathrm{d}t \\ &\quad - \frac{1}{2T^2}\left(\int_0^T \int_0^{t+\phi_0} v_i(s)\mathrm{d}s\,\mathrm{d}t\right)\left(\int_0^T \int_0^{t+\phi_0} v_j(s)\mathrm{d}s\,\mathrm{d}t\right)\end{aligned} \tag{44}$$

Using the change of variable $r = t + \phi_0$, equation (44) can be written as

$$\begin{aligned}\mu_{s_{ij}} &= \frac{1}{2}\left(\frac{1}{T}\int_{\phi_0}^{T+\phi_0} \left(\int_0^r v_i(s)\mathrm{d}s\right)\left(\int_0^r v_j(s)\mathrm{d}s\right)\mathrm{d}r\right. \\ &\quad \left. - \left(\frac{1}{T}\int_{\phi_0}^{T+\phi_0} \int_0^r v_i(s)\mathrm{d}s\,\mathrm{d}r\right)\left(\frac{1}{T}\int_{\phi_0}^{T+\phi_0} \int_0^r v_j(s)\mathrm{d}s\,\mathrm{d}r\right)\right)\end{aligned}$$

Since $v_i(t)$ and $\int v_i(t)\mathrm{d}t$ are T-periodic, and for any T-periodic function $v_i(t)$, $\int_\phi^{T+\phi} v_i(t)\mathrm{d}t = \int_0^T v_i(t)\mathrm{d}t$, the parameter $\mu_{s_{ij}}$ can be written as

$$\mu_{s_{ij}} = \frac{1}{2}\left(\frac{1}{T}\int_0^T\left(\int_0^r v_i(s)\mathrm{d}s\right)\left(\int_0^r v_j(s)\mathrm{d}s\right)\mathrm{d}r - \left(\frac{1}{T}\int_0^T\int_0^r v_i(s)\mathrm{d}s\mathrm{d}r\right)\left(\frac{1}{T}\int_0^T\int_0^r v_j(s)\mathrm{d}s\mathrm{d}r\right)\right)$$

which is the same as μ_{ij}.

Therefore shifting the phase of all the inputs by the same amount ϕ_0 does not change the averaged dynamics in equation (10). But since in general $\kappa_i \neq \kappa_{s_i}$, the initial conditions of the two averaged dynamics may be different. □

Proof of Theorem 6. Using integration by parts, κ_s can be written as

$$\kappa_s = \frac{1}{T}\left(t\int_0^t w(\tau)\mathrm{d}\tau\Big|_0^T - \int_0^T tw(t)\mathrm{d}t\right)$$

Both $v(t)$ and $w(t)$ are T-periodic zero-mean functions. Therefore $\int_0^T w(t)\mathrm{d}t = 0$, and κ_s can be simplified to

$$\kappa_s = -\frac{1}{T}\int_0^T tw(t)\mathrm{d}t$$

Replacing $w(t) = v(t+\phi)$ in the last equation one gets

$$\kappa_s = -\frac{1}{T}\int_0^T tv(t+\phi)\mathrm{d}t$$

which, using $\tau = t+\phi$, can be written as

$$\begin{aligned}\kappa_s &= -\frac{1}{T}\int_\phi^{T+\phi}(\tau-\phi)v(\tau)\mathrm{d}\tau \\ &= -\frac{1}{T}\int_\phi^{T+\phi}\tau v(\tau)\mathrm{d}\tau + \frac{\phi}{T}\int_\phi^{T+\phi}v(\tau)\mathrm{d}\tau\end{aligned}$$

But $\int_\phi^{T+\phi} v(\tau)\mathrm{d}\tau = \int_0^T v(\tau)\mathrm{d}\tau = 0$. Therefore

$$\kappa_s = -\frac{1}{T}\int_\phi^{T+\phi} tv(t)\mathrm{d}t$$

So ϕ_0 is the solution of

$$F(\phi_0) = \int_{\phi_0}^{T+\phi_0} tv(t)\mathrm{d}t = 0$$

which we show always exists. $F(\phi)$ can be written as

$$F(\phi) = \int_0^T tv(t)\mathrm{d}t + \int_T^{T+\phi} tv(t)\mathrm{d}t - \int_0^\phi tv(t)\mathrm{d}t$$

Using change of variable $\tau = t - T$ in the second integral in the right hand side of the expression above

$$F(\phi) = \int_0^T tv(t)\mathrm{d}t + \int_0^\phi (\tau+T)v(\tau+T)\mathrm{d}\tau - \int_0^\phi tv(t)\mathrm{d}t$$

which using $v(\tau+T) = v(\tau)$ can be written as

$$F(\phi) = T\int_0^\phi v(t)\mathrm{d}t + \int_0^T tv(t)\mathrm{d}t$$

Using the results of integration by parts at the beginning of the proof, $F(\phi)$ can be shown as

$$F(\phi) = T\int_0^\phi v(t)\mathrm{d}t - \int_0^T\int_0^t v(\tau)\mathrm{d}\tau\,\mathrm{d}t$$

Defining the constant $M = -\int_0^T\int_0^t v(\tau)\mathrm{d}\tau\,\mathrm{d}t$ and the time-varying parameter $A(t) = \int_0^t v(\tau)\mathrm{d}\tau$, the function $F(\phi)$ can be written as

$$F(\phi) = TA(\phi) - \int_0^T A(t)\mathrm{d}t = TA(\phi) + M$$

Without loss of generality, suppose that $M > 0$. Since $A(0) = A(T) = 0$, therefore $F(0) = F(T) = M > 0$. Though $v(t)$ may be a piecewise continuous function, $A(\phi)$ is continuous everywhere. (It is the area under the t-$v(t)$ curve.) Therefore it is enough to show that there exists $\phi \in [0, T]$ such that $F(\phi) \leq 0$. Also, since $A(\phi)$ is continuous and $A(0) = A(T) = 0$, so $A(\phi)$ has at least one minimum at $\phi = \phi_\mathrm{m}$ and $A(\phi_\mathrm{m}) \leq 0$. Consider $F(\phi_\mathrm{m}) = TA(\phi_\mathrm{m}) - \int_0^T A(t)\mathrm{d}t$. Since $A(t)$ is continuous, using the first mean value theorem for integrals (Salas et al., 2006), there exists $\phi^* \in [0, T]$ such that

$$\int_0^T A(t)\mathrm{d}t = TA(\phi^*)$$

Therefore

$$F(\phi_\mathrm{m}) = T\big(A(\phi_\mathrm{m}) - A(\phi^*)\big)$$

But since $A(\phi_\mathrm{m})$ is the minimum of $A(\phi)$ and T is positive, $F(\phi_\mathrm{m}) \leq 0$, and so there exists $\phi_0 \in [0, T]$ such that $F(\phi_0) = 0$, which results in $\kappa_s = 0$.

Proof of Theorem 10. Using equation (8)

$$\mu_{11}\mu_{22} - \mu_{12}^2 = \frac{1}{4}\left((\lambda_{11} - \kappa_1^2)(\lambda_{22} - \kappa_2^2) - (\lambda_{12} - \kappa_1\kappa_2)^2\right)$$

which using equation (6) and equation (7), and defining $A_i(t) = \int_0^t v_i(t)\mathrm{d}t$, can be written as

$$\begin{aligned}
&\mu_{11}\mu_{22} - \mu_{12}^2 \\
&= \frac{1}{4T^2}\left[\left(\int_0^T A_1^2(t)\mathrm{d}t - \frac{1}{T}\left(\int_0^T A_1(t)\mathrm{d}t\right)^2\right)\right. \\
&\quad \times \left(\int_0^T A_2^2(t)\mathrm{d}t - \frac{1}{T}\left(\int_0^T A_2(t)\mathrm{d}t\right)^2\right) \\
&\quad - \left(\int_0^T A_1(t)A_2(t)\mathrm{d}t - \frac{1}{T}\left(\int_0^T A_1(t)\mathrm{d}t\right)\right. \\
&\quad \left.\left.\times \left(\int_0^T A_2(t)\mathrm{d}t\right)\right)^2\right] \qquad (45)
\end{aligned}$$

For two integrable functions $f, g : [0, T] \to \mathbb{R}$, consider the Cauchy–Bunyakovsky–Schwarz theorem (Mitrinovic et al., 1993: Chapter 4)

$$\left(\int_0^T f^2(x)\mathrm{d}x\right)\left(\int_0^T g^2(x)\mathrm{d}x\right) \geq \left(\int_0^T f(x)\,g(x)\mathrm{d}x\right)^2 \qquad (46)$$

Replacing $f(x)$ with $f(x) - \frac{1}{T}\int_0^T f(x)\mathrm{d}x$, and $g(x)$ with $g(x) - \frac{1}{T}\int_0^T g(x)\mathrm{d}x$ in equation (46) one obtains

$$\begin{aligned}
&\left(\int_0^T f^2(x)\mathrm{d}x - \frac{1}{T}\left(\int_0^T f(x)\mathrm{d}x\right)^2\right) \\
&\quad \times \left(\int_0^T g^2(x)\mathrm{d}x - \frac{1}{T}\left(\int_0^T g(x)\mathrm{d}x\right)^2\right) \\
&\geq \left(\int_0^T f(x)\,g(x)\mathrm{d}x - \frac{1}{T}\left(\int_0^T f(x)\mathrm{d}x\right)\left(\int_0^T g(x)\mathrm{d}x\right)\right)^2 \qquad (47)
\end{aligned}$$

Comparing the right hand side of equation (45) with inequality equation (47) it is evident that the right hand side of equation (45) is always positive, and so $\mu_{11}\mu_{22} \geq \mu_{12}^2$.

For the case when $v_1(t)$ and $v_2(t)$ are square functions with amplitudes B_1 and B_2 respectively, it can be shown that $\mu_{11} = \frac{T^2 B_1^2}{96}$ and $\mu_{22} = \frac{T^2 B_2^2}{96}$. For the case when the relative phase of the two square functions is zero, $\mu_{12} = \sqrt{\mu_{11}\mu_{22}} = \frac{T^2 B_1 B_2}{96}$ and is maximum, and if the phase between them is $\frac{T}{2}$, then $\mu_{12} = -\sqrt{\mu_{11}\mu_{22}} = -\frac{T^2 B_1 B_2}{96}$ and is minimum. For a phase shift $\frac{T}{4}$, $\mu_{12} = 0$. For any other phase, $|\mu_{12}| < \sqrt{\mu_{11}\mu_{22}}$. So using square functions S_{B_1} and S_{B_2} and depending on their relative phase, μ_{12} may have any value in its maximum possible range. Note that one may choose other periodic, zero-mean waveforms, such as sine or triangular functions, to generate μ_{12} in the same range as the square functions, but those other waveforms require bigger amplitudes than the square waves.

Proof of Theorem 11. This proof utilizes the properties stated in the following remark.

Remark 18. *Let n_i and n_j be any natural numbers, i.e. $n_i, n_j \in \mathbb{N}$. Because sinusoids form an orthogonal basis for the Fourier series, the following property holds*

$$\int_0^T \cos(\Omega n_i t)\cos(\Omega n_j t)\mathrm{d}t = \int_0^T \sin(\Omega n_i t)\sin(\Omega n_j t)\mathrm{d}t = \begin{cases} 0 & \text{if } n_i \neq n_j \\ \pi/\Omega & \text{if } n_i = n_j \end{cases}$$

Additionally

$$\int_0^T \cos(\Omega n_i t)\sin(\Omega n_j t)\mathrm{d}t = 0$$

for any $n_i, n_j \in \mathbb{N}$.

Let the input waveforms be defined as finite Fourier series as in Equation (32). Thus

$$\begin{aligned}
\kappa_i &= \frac{1}{T}\int_0^T \int_0^t v_i(\tau)\mathrm{d}\tau\,\mathrm{d}t \\
&= \frac{1}{T}\int_0^T \int_0^t \Omega \sum_{n=1}^{l}\left(a_{i,n}\cos(\Omega n\tau) + b_{i,n}\sin(\Omega n\tau)\right)\mathrm{d}\tau\,\mathrm{d}t
\end{aligned}$$

Because $\Omega/T = 2\pi/T^2$, the previous expression can be shown to be equivalent to

$$\kappa_i = \frac{2\pi}{T^2}\sum_{n=1}^{l}\left(a_{i,n}\underbrace{\frac{1}{T}\int_0^T\int_0^t \cos(\Omega n\tau)\mathrm{d}\tau\,\mathrm{d}t}_{=0} + b_{i,n}\underbrace{\frac{1}{T}\int_0^T\int_0^t \sin(\Omega n\tau)\mathrm{d}\tau\,\mathrm{d}t}_{=\frac{T^2}{2\pi n}}\right)$$

Thus

$$\kappa_i = \sum_{n=1}^{l}\frac{b_{i,n}}{n} \qquad (48)$$

Prior to defining μ_{ij} as in Theorem 11, it is necessary to compute λ_{ij} (see equation (7)) because μ_{ij} is defined using λ_{ij} as shown in equation (8). Let v_i and v_j be defined as finite Fourier series, i.e.

$$v_i(t) = \Omega \sum_{n_i=1}^{l} \left(a_{i,n_i} \cos(\Omega n_i \tau) + b_{i,n_i} \sin(\Omega n_i \tau) \right)$$

$$v_j(t) = \Omega \sum_{n_j=1}^{l} \left(a_{j,n_j} \cos(\Omega n_j \tau) + b_{j,n_j} \sin(\Omega n_j \tau) \right)$$

It can be shown that

$$\lambda_{ij} = \frac{1}{T} \int_0^T \left(\int_0^t v_i(s_i) \mathrm{d}s_i \right) \left(\int_0^t v_j(s_j) \mathrm{d}s_j \right) \mathrm{d}t$$

is equivalent to

$$\begin{aligned} \lambda_{ij} = \frac{1}{T} \int_0^T \sum_{n_i, n_j=1}^{l} \Bigg(& \frac{a_{i,n_i} a_{j,n_j}}{n_i n_j} \sin(\Omega n_i t) \sin(\Omega n_j t) \\ & + \frac{a_{i,n_i} b_{j,n_j}}{n_i n_j} \sin(\Omega n_i t) - \frac{a_{i,n_i} b_{j,n_j}}{n_i n_j} \sin(\Omega n_i t) \cos(\Omega n_j t) \\ & + \frac{b_{i,n_i} a_{j,n_j}}{n_i n_j} \cos(\Omega n_i t) \sin(\Omega n_j t) + \frac{b_{i,n_i} b_{j,n_j}}{n_i n_j} \cos(\Omega n_i t) \\ & - \frac{b_{i,n_i} b_{j,n_j}}{n_i n_j} \cos(\Omega n_i t) \cos(\Omega n_j t) + \frac{b_{i,n_i} a_{j,n_j}}{n_i n_j} \sin(\Omega n_j t) \\ & + \frac{b_{i,n_i} b_{j,n_j}}{n_i n_j} - \frac{b_{i,n_i} b_{j,n_j}}{n_i n_j} \cos(\Omega n_j t) \Bigg) \mathrm{d}t \end{aligned}$$

Switching the order of integration and summation and applying the properties from Remark 18 yields

$$\lambda_{ij} = \frac{1}{2} \sum_{n=1}^{l} \left(\frac{1}{n^2} \left(a_{i,n} a_{j,n} + b_{i,n} b_{j,n} \right) \right) + \sum_{n_i, n_j=1}^{l} \left(\frac{b_{i,n_i} b_{j,n_j}}{n_i n_j} \right) \tag{49}$$

Notice that

$$\kappa_i \kappa_j = \sum_{n_i, n_j=1}^{l} \left(\frac{b_{i,n_i} b_{j,n_j}}{n_i n_j} \right)$$

Therefore

$$\mu_{ij} = \frac{1}{2} \left(\lambda_{ij} - \kappa_i \kappa_j \right) = \frac{1}{4} \sum_{n=1}^{l} \left(\frac{1}{n^2} \left(a_{i,n} a_{j,n} + b_{i,n} b_{j,n} \right) \right) \tag{50}$$

Proof of Theorem 16. Consider the problem of minimizing the input energy of $v_i(t)$ with $\mu_{ii} = \mu^\star$, which satisfies the constraint in equation (22). Assume that $v_i(t)$ is a continuous, zero-mean, T-periodic function. Therefore $v_i(t)$ can be expressed as a Fourier series, i.e.

$$v_i(t) = \Omega \sum_{n=1}^{\infty} \left(a_{i,n} \cos(\Omega n t) + b_{i,n} \sin(\Omega n t) \right)$$

Since $v_i(t)$ is defined as a Fourier series, one finds that

$$\mu_{ii} = \mu^\star = \frac{1}{4} \sum_{n=1}^{\infty} \frac{1}{n^2} \left(a_{i,n}^2 + b_{i,n}^2 \right) \tag{51}$$

and the input energy of this waveform is

$$\| v_i(t) \|_{T,2}^2 = \frac{\Omega^2}{2} \sum_{n=1}^{\infty} \left(a_{i,n}^2 + b_{i,n}^2 \right) \tag{52}$$

Notice that the summands of equation (51) and equation (52) differ only by a factor of $1/n^2$. Minimizing equation (52) subject to equation (51) is equivalent to minimizing $\sum_{n=1}^{\infty} (a_{i,n}^2 + b_{i,n}^2)$ subject to $\sum_{n=1}^{\infty} \frac{1}{n^2} (a_{i,n}^2 + b_{i,n}^2) = \mu^\star$. Notice that

$$\begin{aligned} \sum_{n=1}^{\infty} \left(a_{i,n}^2 + b_{i,n}^2 \right) & = \sum_{n=1}^{\infty} \left(\frac{1}{n^2} \left(a_{i,n}^2 + b_{i,n}^2 \right) + \frac{n^2 - 1}{n^2} \left(a_{i,n}^2 + b_{i,n}^2 \right) \right) \\ & = \sum_{n=1}^{\infty} \left(\frac{1}{n^2} \left(a_{i,n}^2 + b_{i,n}^2 \right) \right) + \sum_{n=1}^{\infty} \left(\frac{n^2 - 1}{n^2} \left(a_{i,n}^2 + b_{i,n}^2 \right) \right) \end{aligned}$$

Applying the constraint yields

$$\sum_{n=1}^{\infty} \left(a_{i,n}^2 + b_{i,n}^2 \right) = \mu^\star + \sum_{n=1}^{\infty} \left(\frac{n^2 - 1}{n^2} \left(a_{i,n}^2 + b_{i,n}^2 \right) \right)$$

Since $\mu^\star$ is a constant and $(n^2 - 1)/n^2 = 0$ if $n = 1$, minimizing the input energy of $v_i(t)$ subject to $\mu_{ii} = \mu^\star$ is equivalent to minimizing

$$\sum_{n=2}^{\infty} \frac{n^2 - 1}{n^2} \left(a_{i,n}^2 + b_{i,n}^2 \right) \tag{53}$$

Notice that $(n^2 - 1)/n^2 > 0$ for all $n > 1$, so the minimum of equation (53) occurs when $a_{i,n}^2 + b_{i,n}^2 = 0$ for all $n \geq 2$ which occurs when $a_{i,n}, b_{i,n} = 0$ for all $n \geq 2$.

Therefore, the minimum-input-energy, continuous, zero-mean, T-periodic waveform corresponding to $\mu_{ii} = \mu^{\star}$ can be expressed as a Fourier series where all of the Fourier coefficients except for the first pair are zero. Such a Fourier series represents a sinusoid, i.e.

$$v_i(t) = b_i \Omega \cos(\Omega t + \phi_i) = \Omega \sum_{n=1}^{\infty} \left(a_{i,n} \cos(\Omega n t) + b_{i,n} \sin(\Omega n t) \right)$$

where $a_{i,1} = b_i \cos(-\phi_i)$, $b_{i,1} = b_i \sin(-\phi_i)$, and $a_{i,n}, b_{i,n} = 0$ for all $n > 1$. Thus, the minimum-input-energy, continuous, zero-mean, T-periodic waveform corresponding to $\mu_{ii} = \mu^{\star}$ is a sinusoid.

Assume that $\boldsymbol{v}(t) = [v_1(t), \ldots, v_m(t)]^T$ is a vector of continuous, zero-mean, T-periodic input waveforms satisfying the conditions in equation (22). This assumption constrains the possible input waveforms $v_i(t)$ such that each input waveform has a prescribed value of μ_{ii}. Furthermore, each pair of input waveforms has a prescribed value of μ_{ij}.

The input energy of $\boldsymbol{v}(t)$, $\left\| v(t) \right\|_{T,2}^{2}$, does not depend on the relative phase of the input waveforms, which determines μ_{ij}. Thus, the optimization problem reduces to minimizing the input energy of each $v_i(t)$ with μ_{ii} satisfying equation (22).

As previously stated, for $v_i(t)$ with μ_{ii} satisfying equation (22) the minimum-input-energy input waveform corresponds to sinusoids. Therefore, if $\boldsymbol{v}(t) = [v_1(t), \ldots, v_m(t)]^T$ is a vector of continuous, zero-mean, T-periodic input waveforms satisfying the conditions in equation (22), the minimum input energy corresponds to sinusoidal input waveforms, i.e. $v_i(t) = B_i \Omega \cos(\Omega t + \phi_i)$. □